Environmental Science and Pollution Research (2026) 33:7498–7516
https://doi.org/10.1007/s11356-026-37770-4

RESEARCH ARTICLE

Burkholderia sp. ZF6-mediated mitigation of Cd and Zn stress in contaminated soil: effects on Chinese cabbage growth and rhizosphere microbial communities

Soo Yeon Lee[1] · **Kyung-Suk Cho**[1]

Received: 30 December 2025 / Accepted: 19 April 2026 / Published online: 30 April 2026
© The Author(s) 2026

Abstract
This study investigated the effects of *Burkholderia* sp. ZF6, a plant growth-promoting bacterium with heavy metal resistance genes (*cad*A and *znt*A), on the growth of Chinese cabbage (*Brassica rapa* subsp. *pekinensis*) and cadmium (Cd)/zinc (Zn) removal in contaminated soils. ZF6 inoculation significantly increased root biomass (over twofold) and enhanced soil Cd and Zn removal efficiencies by approximately 2–4 times (19.9% for Cd and 11.5% for Zn). The abundance of *cad*A and *znt*A genes increased by 1.2–2.7 times, suggesting an enrichment of heavy metal-resistant microbial populations. Microbial community analysis showed that ZF6 inoculation reshaped the rhizosphere microbiome, increasing the relative abundance of genera such as *Klebsiella*, *Agrobacterium*, *Burkholderia*, *Sphingomonas,* and *Pseudomonas*. Notably, the abundance of *Burkholderia*, corresponding to ZF6, exhibited an increasing trend over time. Network analysis further indicated that microbial interactions became more complex in ZF6-treated soils (1.7–4.5-fold higher connectivity). Correlation analysis revealed that *znt*A abundance was associated with selected functional genes (e.g., K04565 and K01534) and inversely related to soil Cd concentration, suggesting a potential link between microbial functional potential and metal dynamics. Overall, ZF6 inoculation facilitated the restructuring of soil microbial communities to favor heavy metal-resistant bacteria. These findings highlight the potential of ZF6 as a scalable microbial-assisted phytoremediation strategy, although further validation under field conditions is required.

Keywords *Burkholderia* sp. ZF6 · Chinese cabbage · Heavy metal tolerance genes · Plant growth promotion · Phytoremediation · Soil bacterial community

Introduction

Certain trace metals, such as copper (Cu), zinc (Zn), and nickel (Ni), are essential for bacterial metabolic processes in soil, whereas highly toxic metals such as cadmium (Cd) pose significant environmental threats and can severely impact microbial diversity (Khatoon et al. 2024). In response, bacteria in contaminated soils have developed resistance mechanisms, including metal complexation, efflux transport, and gene regulation systems for detoxification (Bazzi et al. 2020; Halder et al. 2022). These resistance traits can spread via horizontal gene transfer (HGT) and mobile genetic elements, contributing to the persistence of metal resistance in soil ecosystems (Gendy et al. 2020; Halder et al. 2022). Heavy metal-resistant bacteria also play an important role in promoting plant growth under stress conditions (Liu et al. 2024a). Previous studies have demonstrated that inoculation with strains such as *Citrobacter werkmanii*, *Enterobacter cloacae*, and *Bacillus* sp. enhances plant growth and metal uptake in contaminated soils (Ajmal et al. 2022; Wang et al. 2022). In particular, plant growth-promoting bacteria (PGPB), including *Burkholderia* and *Pseudomonas*, contribute to phytoremediation by improving metal bioavailability, alleviating stress, and enhancing plant growth (Ajmal et al. 2022; Wang et al. 2022). However, most studies have primarily focused on plant-level responses, whereas the interactions between inoculated PGPB and native soil

Responsible Editor: Diane Purchase

✉ Kyung-Suk Cho
kscho@ewha.ac.kr

[1] Department of Environmental Science & Engineering, Ewha Womans University, 52, Ewhayeodae-Gil, Seodaemun-Gu, Seoul 03760, Republic of Korea

microbial communities remain insufficiently understood (Dobrzyński et al. 2025). In particular, the ecological impacts of microbial inoculation under multi-metal stress and the dynamics of resistance genes (e.g., *cadA* and *zntA*) in the rhizosphere have been rarely explored (Niegowska et al. 2021; McCorquodale-Bauer et al. 2025). Addressing these gaps is essential for improving the effectiveness and sustainability of phytoremediation strategies.

Therefore, this study aims to explore how ZF6 alleviates Cd/Zn stress and promotes plant growth by regulating microbial communities and functional genes in the rhizosphere. This study uses multi-omics analysis to show how *Burkholderia* sp. ZF6 enhances plant growth, alters microbial communities, and increases functional gene expression. *Burkholderia* sp. ZF6, a heavy metal-resistant PGPB isolated from forest soil, was used as the inoculant strain (Lee and Cho 2025). ZF6 exhibits robust heavy metal resistance through two key genetic systems. In particular, ZF6 was selected in this study due to its previously demonstrated high tolerance to Cd and Zn stress and its possession of both *cad*A and *znt*A genes, which are key determinants of metal resistance and transport in bacteria. It also has various plant growth-promoting abilities, such as indole-3-acetic acid (IAA) production, phosphate solubilization, and siderophore activity. Due to these multifunctional properties, ZF6 has the potential to play an important role in improving phytoremediation efficiency in polluted soils. Compared to previously reported *Burkholderia* strains, which often exhibit either plant growth-promoting traits or metal resistance individually, ZF6 uniquely combines multiple functional traits, including metal resistance, phytohormone production, and nutrient solubilization, suggesting its potential for synergistic effects in phytoremediation (Gamalero and Glick 2024; Liu et al. 2024a). Furthermore, Chinese cabbage (*Brassica rapa* subsp. *pekinensis*) was selected as the model plant due to its rapid growth, high biomass production, and known capacity for heavy metal accumulation, making it suitable for evaluating phytoremediation efficiency under controlled conditions (Bortoloti and Baron 2022; Liao et al. 2023). These characteristics make the ZF6–Chinese cabbage system an appropriate model for investigating microbe–plant interactions and their combined effects on heavy metal removal and soil microbial dynamics.

This study evaluates the effects of ZF6 inoculation in Cd- and Zn-contaminated soils by assessing plant growth, heavy metal removal, soil microbial community structure, plant growth-promoting activities, and the abundance of resistance-related genes. We hypothesize that ZF6 inoculation will (i) enhance plant growth and metal uptake, (ii) reshape microbial communities toward beneficial and metal-resistant taxa, and (iii) increase the abundance of functional genes associated with heavy metal resistance.

Materials and methods

Experimental design

A pot experiment was conducted under controlled growth chamber conditions to investigate the effects of *Burkholderia* sp. ZF6 inoculation on Chinese cabbage growth, Cd and Zn removal in rhizosphere soils, and rhizosphere microbial responses. The experimental design consisted of two treatments: (i) a non-inoculated control (Chinese cabbage only) and (ii) a ZF6-inoculated treatment. Each treatment was performed in triplicate. Plants were cultivated in Cd- and Zn-contaminated soil for 40 days. Soil and plant samples were collected at 0 (initial), 20, and 40 days to assess plant growth parameters, soil and plant heavy metal concentrations, rhizosphere microbial community structure, and functional gene profiles.

Preparation of heavy metal-contaminated soil

Solutions of 100 mg·L^{-1} Cd and 2000 mg·L^{-1} Zn were prepared using $CdCl_2 \cdot H_2O$ and $ZnSO_4 \cdot 7H_2O$ reagents, respectively (Raza et al. 2020; Taeprayoon et al. 2024). Each heavy metal solution was sterilized using a 0.45-μm sterile filter and syringe. A total of 20 kg of soil for plant cultivation (Shinsung Mineral Co., Goesan, Chungcheongbuk-do, South Korea) was thoroughly mixed with 100 mL of each heavy metal solution. The contaminated soil was then divided into two portions, sterilized at a low temperature (100 °C, 1 h), and stored in a dark, cool place for 24 h before use in the experiments. Although heat sterilization may alter or reduce native soil microbial communities, this approach was applied to minimize background microbial variability and to better isolate the effects of ZF6 inoculation under controlled conditions. Therefore, the experimental design was intended to evaluate the relative impact of the inoculated strain rather than to fully represent natural soil ecosystems. The physicochemical properties of the soil prior to contamination were characterized to ensure reproducibility. The soil was classified as sandy loam, with an initial pH of 6.85 ± 0.05 and organic matter content of 23.44 ± 0.13%. These baseline properties were considered important factors influencing microbial activity and metal mobility. The background heavy metal concentration (Arsenic (As), Cd, Cu, Ni, Pb and Zn) in the soil was investigated and found to be 4.29 ± 0.04 mg-As·kg-$soil^{-1}$, 0.06 ± 0.01 mg-Cd·kg-$soil^{-1}$, 5.72 ± 0.01 mg-Cu·kg-$soil^{-1}$, 7.27 ± 0.03 mg-Ni·kg-$soil^{-1}$, 10.28 ± 0.08 mg-Pb·kg-$soil^{-1}$, and 38.24 ± 0.02 mg-Zn·kg-$soil^{-1}$. After contamination, the initial soil contamination concentrations were 71.76 ± 20.96 mg-Cd·kg-$soil^{-1}$ and 1683.36 ± 175.85 mg-Zn·kg-$soil^{-1}$.

Plant cultivation and ZF6 inoculation

Seedlings of Chinese cabbage, a species known for its tolerance to stress conditions and classification as a heavy metal hyperaccumulator, were planted in contaminated soil-filled pots, with eight seedlings per pot (Byunsan Seedling Farm, Buan, Jeollabuk-do, South Korea) (Małecka et al. 2021). *Burkholderia* sp. ZF6 was cultured in 1/10 LB medium at 35 °C and 130 rpm for two days (Lee and Cho 2025). The cultured cells were collected by centrifugation (13,000 rpm, 10 min), washed with sterile water, and resuspended in sterile water to achieve an OD_{600} of 0.6 (approximately 10^8 CFU·mL^{-1}). The bacterial suspension was applied directly to the rhizosphere to ensure effective colonization. Inoculation was performed once at the beginning of the experiment, and uniform distribution was achieved by carefully applying the suspension around the root zone. Details on the isolation of ZF6, its heavy metal resistance, and its plant growth-promoting (PGP) properties have been presented in previous studies (Lee and Cho 2025), while additional data on ZF6 growth under varying metal concentrations and its metal adsorption capacity are provided in the Supplementary Materials (Table S1, Figs. S1 and S2).

Plastic pots (W 59 cm × L 33 cm × H 18 cm) were prepared by layering 1–2 cm of coarse gravel at the bottom for drainage and filling each pot with 10 kg of contaminated soil. A 100 mL suspension of ZF6 cells was applied around the roots of the Chinese cabbage seedlings in each pot. For the untreated control pots, 100 mL of distilled water was added instead. The pots were placed in an indoor plant incubator (VS-5GC, Vision Scientific Co., Ltd., South Korea) for a 40-day experiment. Water was added every 3 days to prevent soil desiccation.

Soil sampling and analysis of physical and chemical properties

At 20 and 40 days, loosely attached soil was removed by gently shaking the root system. In addition to the soil tightly adhering to the root surface, soil located in the immediate root-adjacent zone (within a few millimeters of the root surface) was also collected by gentle brushing and manual sampling. This combined fraction was operationally defined as rhizosphere soil. Approximately 100 g of soil was collected, air-dried for more than 12 h, and sieved through a 2-mm mesh. Portions of the soil samples were stored at 4 °C for residual heavy metal concentration and enzyme activity analysis and at − 23 °C for DNA extraction and microbial community analysis. The physical and chemical properties of the sieved soil were analyzed according to the Soil Pollution Process Test Methods (Korean Ministry of Environment 2018).

Soil pH was measured by mixing 5 g of soil with 25 mL of distilled water at room temperature, allowing the mixture to settle for 30 min, and measuring the pH with a pH meter (420A, Thermo Orion, USA). Moisture content was determined by drying 2 g of soil in a constant-temperature oven (VS-4150ND, Vision Scientific Co., Ltd., South Korea) at 110 °C until a constant weight was achieved, then calculating the percentage relative to the dry weight. Organic matter content was measured by placing the dried soil in a crucible, igniting it in a muffle furnace (DH.WF11.27 Furnace, DAIHAN Scientific Co., Ltd., South Korea) at 550 °C for 1 h, and calculating the percentage relative to the dry weight.

Analysis of total heavy metal concentration in soil

Soil samples stored at 4 °C were dried at 110 °C for 4 h, finely ground using a mortar and pestle, and used for heavy metal analysis. The total Cd and Zn concentrations in the contaminated soil were determined by modifying the USEPA 3050B method and previously described protocols (Mapanda et al. 2005; Huang et al. 2007; Long et al. 2021; Yahaya et al. 2021). Heavy metal concentrations were quantified using an inductively coupled plasma mass spectrometer (ICP-MS) (7850 ICP-MS, Agilent, USA). A standard calibration curve was established using Cd and Zn solutions ranging from 0 to 100 mg/L to determine metal concentrations. The heavy metal removal efficiency was calculated using the following equation:

$$\text{Removal efficiency}(\%) = \frac{C_i - C_e}{C_i} \times 100$$

where C_i represents the initial concentration of the total Cd and Zn concentrations in the contaminated soil (mg·kg-soil^{-1}), and C_e represents the concentration of the total Cd and Zn concentrations in the contaminated soil after cultivation (mg·kg-soil^{-1}).

Evaluation of IAA, phosphatase, and siderophore activity of soil

The production of IAA, a key plant growth-promoting hormone, was assessed as described by Benitez et al. (Benitez et al. 2004). Two grams of soil were placed in a conical flask and mixed with 6 mL of phosphate buffer (pH 7.5) containing 1% (w/v) glucose and 4 mL of 0.06% (w/v) L-tryptophan solution. For the control group, triple-distilled water was used instead of L-tryptophan. After incubation at 37 °C in the dark for 24 h, the mixture was transferred to a 15 mL centrifuge tube and centrifuged at 4000 rpm for 5 min. Three milliliters of the supernatant were transferred to a test tube, and 2 mL of Salkowski's reagent (composed of 98 mL $HClO_4$ (35%, v/v) and 2 mL 0.2 M $FeCl_3 \cdot 6H_2O$)

was added. After incubation at 25 °C in the dark for 30 min, the resulting red color was measured at 535 nm.

Phosphatase activity, which facilitates phosphorus hydrolysis in soil (Chen et al. 2024; Campdelacreu Rocabruna et al. 2024), was evaluated by mixing 1 g of soil with 4 mL of Modified Universal Buffer (MUB), 0.25 mL of toluene, and 1 mL of 0.115 M *p*-nitrophenyl phosphate hexahydrate (PNP) solution in a conical flask. The MUB solution contained 12.1 $g{\cdot}L^{-1}$ Tris-hydroxymethyl aminomethane (THAM), 11.6 $g{\cdot}L^{-1}$ maleic acid, 14.0 $g{\cdot}L^{-1}$ citric acid, and 6.6 $g{\cdot}L^{-1}$ boric acid, all dissolved in 1 N NaOH and adjusted to pH 6.5 with 0.1 N HCl. For the control group, distilled water was used instead of the PNP solution. Following 24-h incubation at 37 °C, 1 mL of 0.5 M $CaCl_2{\cdot}2H_2O$ and 4 mL of 0.5 M NaOH were added, mixed, and centrifuged at 4,000 rpm for 5 min. The resulting pale yellow supernatant was measured at 400 nm.

Siderophore secretion, which acts as a heavy metal chelator, was analyzed following Hwang and Song (2020) and Nagarajkumar et al. (2004). Soil samples were inoculated with 20 mL of sterile nutrient broth (NB) containing 1 $g{\cdot}L^{-1}$ meat extract, 5 $g{\cdot}L^{-1}$ peptone, 5 $g{\cdot}L^{-1}$ sodium chloride, and 2 $g{\cdot}L^{-1}$ yeast extract, then incubated at 30 °C with shaking (120 rpm) for 24 h. For the control group, distilled water was used instead of NB. After incubation, 14 mL of the culture medium was centrifuged at 4000 rpm for 5 min, and 10 mL of the supernatant was adjusted to pH 2–3 using 1 M HCl. For siderophore extraction, an equal volume of ethyl acetate was added to the supernatant mixed with 1 M HCl. After phase separation, 2 mL of the upper organic layer was transferred to a test tube and mixed with Hathway reagent (containing 1 mL of 0.1 M potassium ferricyanide, 1 mL of 0.1 M $FeCl_3$ in 0.1 M HCl, and 98 mL of distilled water). The resulting bluish-green solution was incubated at 30 °C in the dark for 30 min, and absorbance was measured at 700 nm.

Plant sample collection and analysis

After collecting rhizosphere soil, the plants were gently washed under running tap water to remove any remaining debris. The number of leaves on each plant was counted, and chlorophyll content was measured using a chlorophyll meter after removing surface moisture from the leaves. Plant length was recorded in centimeters after air-drying at room temperature as much as possible, and fresh weight was measured using an electronic scale (WBA-220, DAIHAN Scientific Co., Ltd., South Korea). For biomass analysis, dry weight was determined after drying the samples in a constant-temperature oven (VS-4150ND, Vision Scientific Co., Ltd., South Korea) at 70 °C for 72 h.

For heavy metal analysis, 0.2 g of dried plant stems and roots were separately treated with 2 mL of 30% (v/v) H_2O_2 as the first extraction solution and heated on a hot plate (DH. WHP03024, DAIHAN Scientific, South Korea) at 150 °C for 30 min to facilitate decomposition. Next, 2 mL of nitric acid was added as the second extraction solution and heated under the same conditions for another 30 min. Finally, 2 mL of perchloric acid was added as the third extraction solution and subjected to identical heating conditions. Between each step, distilled water was used to evaporate the previous acid solution completely by heating at 130 °C for 4 h. After cooling to room temperature, the digested samples were transferred to a 50 mL test tube and diluted with a 5% (v/v) nitric acid solution. Heavy metal concentrations in plant samples were quantified using ICP-MS, following the same procedure as for soil heavy metal analysis.

DNA extraction of functional genes and quantitative real-time polymerase chain reaction

Pretreated soil samples were thawed before DNA extraction. A 0.3 g portion of thawed soil was then placed in a 1.5 mL microcentrifuge tube, and genomic DNA (gDNA) was extracted using the NucleoSpin® Soil Kit (Macherey–Nagel, Germany) and the BeadBeater (MP, FastPrep 24 Homogenizer) according to the manufacturer's instructions. The gDNA was eluted with 50 µL of elution buffer and quantified using a SpectraMax QuickDrop Spectrophotometer (Molecular Devices, San Jose, CA, USA). The extracted gDNA was stored at − 23 °C until analysis. To compare the abundance of functional genes in soil, quantitative real-time polymerase chain reaction (qPCR) was performed to quantify total bacterial 16S rRNA, *cad*A, and *znt*A genes (Manzoor et al. 2019; Lee et al. 2021). The 16S rRNA gene was amplified using primers 340 F (5′-TCC TAC GGG AGG CAG CAG-3′) and 805R (5′-GAC TAC HVG GGT ATC TAA TCC-3′) (Lee et al. 2021), while primers for the *cad*A and *znt*A genes were obtained from previous studies (Manzoor et al. 2019). The qPCR reaction mixture consisted of 2 µL of DNA template, 1 µL of each primer (10 µM), and 10 µL of SYBR Green qPCR Master Mix 2X (BioFact, South Korea), with sterile distilled water added to a final volume of 20 µL. The PCR conditions consisted of a pre-denaturation step at 95 °C for 15 min, followed by 35 cycles of denaturation at 95 °C for 20 s, annealing at 50 °C for 40 s, and extension at 72 °C for 30 s. The final reading step was performed at 82 °C for 30 s. The qPCR was conducted using the CFX96™ Real-Time System (Bio-Rad Laboratories, Hercules, CA, USA). A standard curve for quantitative detection was generated using the *Escherichia coli* 16S rRNA gene as a reference (Lee et al. 2021). DNA standards ranging from 10^3 to 10^9 gene copies were used, and the standard curve is shown in Fig. S3b. Relative expression of the *cad*A and *znt*A genes was quantified using the comparative Ct method ($2^{-\Delta\Delta Ct}$ method) (Schmittgen and Livak 2008).

Soil bacterial community analysis

The soil bacterial community was analyzed using the Illumina MiSeq platform, following the method described by Lee et al. (Lee et al. 2023). A 0.3 g soil sample was transferred into a 1.5-mL microcentrifuge tube, and gDNA was extracted using the NucleoSpin® Soil Kit (Macherey–Nagel, Germany) and a BeadBeater (MP, FastPrep 24 Homogenizer), according to the manufacturer's instructions. The gDNA was eluted in 50 µL of elution buffer and quantified using a SpectraMax QuickDrop Spectrophotometer (Molecular Devices, San Jose, CA, USA). The extracted gDNA was stored at − 20 °C until further analysis. For bacterial community profiling, a two-step PCR was performed using a T100™ Thermal Cycler (Bio-Rad Laboratories, USA). The first PCR targeted the 16S rRNA gene using the amplicon-515F (5′-TCG TCG GCA GCG TCA GAT GTG TAT AAG AGA CAG GTG CCA GCM GCC GCG GTA A-3′) and amplicon-806R (5′-GTC TCG TGG GCT CGG AGA TGT GTA TAA GAG ACA GGG ACT ACH VGG GTW TCT AAT-3′) primer pair. Each primer contained a 5′ pre-adapter, sequencing primer sequence, and a V4 region-specific target sequence. The PCR reaction mixture included 2 µL of DNA template, 1 µL of each primer (10 µM), 4 µL of dNTPs (2.5 mM), 5 µL of 10 × PCR buffer with $MgCl_2$, and 0.25 µL of Taq polymerase (Genenmed Inc., Seoul, South Korea), with sterile distilled water added to a final volume of 50 µL. The PCR thermal profile consisted of a pre-denaturation step at 94 °C for 3 min; 35 cycles of denaturation at 94 °C for 30 s, annealing at 55 °C for 30 s, and extension at 72 °C for 30 s; followed by a final extension at 72 °C for 5 min. The amplification product was verified via electrophoresis on a 1.5% agarose gel.

In the second PCR round, index primers (index1 N7XX and index2 S5XX) from a Nextera XT Index Kit (FC-131–1001, Illumina Inc., CA, USA) were used according to the manufacturer's protocol. The index primer sequences for N7XX and S5XX were 5′-CAAGCAGAAGACGGC ATACGAGAT-XXXXXXX-GTCTCGTGGGCTCGG-3′ and 5′-AATGATACGGCGACCACCGAGATCTACAC-XXXXXXX-TCGTCGGCAGCGTC-3′, respectively. Each primer consisted of an adapter sequence, a multiplex identifier tag, and a pre-adapter sequence. The PCR mixtures were prepared in the same way as for the first reaction, and the thermal profile included an initial denaturation at 95 °C for 3 min, followed by 30 cycles of 95 °C for 30 s, 55 °C for 30 s, and 72 °C for 30 s, with a final extension at 72 °C for 5 min. The amplified products were visualized on 2% melting agarose gels and purified using a QIAquick Gel Extraction Kit (Qiagen Inc., Valencia, CA, USA). Purified amplicons were pooled and submitted to Macrogen Inc. (Seoul, South Korea) for sequencing using an Illumina MiSeq platform (Illumina Inc.).

Raw sequences were processed using QIIME software (version 1.9). Adapter sequences were removed using Fastp, and paired-end reads were merged with FLASH (version 1.2.11). Only merged reads between 200 and 400 bp were retained; sequences outside this range were discarded. Sequencing data were deposited in the NCBI Sequence Read Archive (SRA) database (accession number: SRP352503). To identify bacterial biomarkers influenced by untreated conditions or ZF6 inoculation in Chinese cabbage rhizosphere samples, linear discriminant analysis effect size (LEfSe) was performed at the genus level, using data collapsed to that taxonomic rank. Statistical analysis was conducted using the Kruskal–Wallis test, with an LDA score threshold of ≥ 4.0 (Duan and Li 2023). Functional changes in the microbial community in response to environmental variables were inferred using PICRUSt2 based on 16S rRNA gene data, with annotations derived from the Kyoto Encyclopedia of Genes and Genomes (KEGG) database (Wang et al. 2021; Duan and Li 2023). These predictions represent potential functional profiles rather than direct measurements of gene expression. Data visualization and statistical tests ($p < 0.05$) were conducted using the STAMP software (Duan and Li 2023). To ensure reproducibility and comparability among samples, sequencing depth was normalized across all samples prior to downstream analysis (Duan and Li 2023). Quality filtering, chimera removal, and OTU clustering were conducted using standardized pipelines, and all parameters were applied consistently across treatments.

Statistical analysis

All results are presented as the mean of three replicates. Significant differences between mean values were determined using one-way analysis of variance (ANOVA), followed by Bonferroni post-hoc tests at a confidence level of $p < 0.05$. Variation partitioning analysis (VPA) was conducted using R (version 4.0.1) to evaluate the relative contributions of ZF6 inoculation, heavy metal contamination, and PGP enzyme activity in soil. Co-occurrence network analysis was used to assess changes in microbial connectivity patterns influenced by ZF6 inoculation, with significance set at $p < 0.01$. Network topology and graphical visualizations were generated using the open-source software Gephi (version 0.9.2). Analyses were primarily performed using the "phyloseq," "vegan," and "microeco" packages in R. A heatmap showing the classification of soil bacterial communities was generated in R, and cluster analysis based on principal component analysis (PCA) was conducted using the "FactoMineR" package (Lee et al. 2023). Additionally, network analysis incorporating soil heavy metal concentrations, plant growth-promoting enzyme activity (IAA, phosphatase, and siderophore), and microbial communities was performed using extended local similarity analysis (eLSA).

Local similarity (LS) values and corresponding *p*-values were calculated, and the resulting networks were visualized using Cytoscape (version 3.9.1) (Lee et al. 2023).

Results

Effects of ZF6 inoculation on Chinese cabbage growth and PGP abilities of soil microorganisms

The effects of ZF6 inoculation on Chinese cabbage growth are shown in Fig. S4. Shoot length did not differ significantly among treatments, whereas root biomass showed a clear increasing trend under ZF6 inoculation over time. Root length and shoot biomass increased during the experiment; however, these changes were not significantly different between treatments. In contrast, root biomass increased in ZF6-inoculated treatments but decreased in non-inoculated soils, indicating a treatment-specific response. At day 40, chlorophyll content and leaf number were slightly higher (approximately 1.1-fold) in ZF6-inoculated treatments. Correlation analysis showed generally weak to moderate relationships between ZF6 inoculation and plant growth parameters (Fig. 1). Among these, only root biomass showed a statistically significant positive correlation ($r = 0.33$, $p = 0.045$), while other parameters were not significant. The PGP abilities of soil microorganisms during phytoremediation in Cd- and Zn-contaminated soil are presented in Fig. 2. IAA production and phosphatase activity increased under ZF6 inoculation, particularly after 20 days, whereas siderophore production did not show a consistent inoculation effect (Fig. 2a and b). IAA production was significantly higher in ZF6-inoculated treatments after 20 days, and phosphatase activity showed a sustained increase over time. In

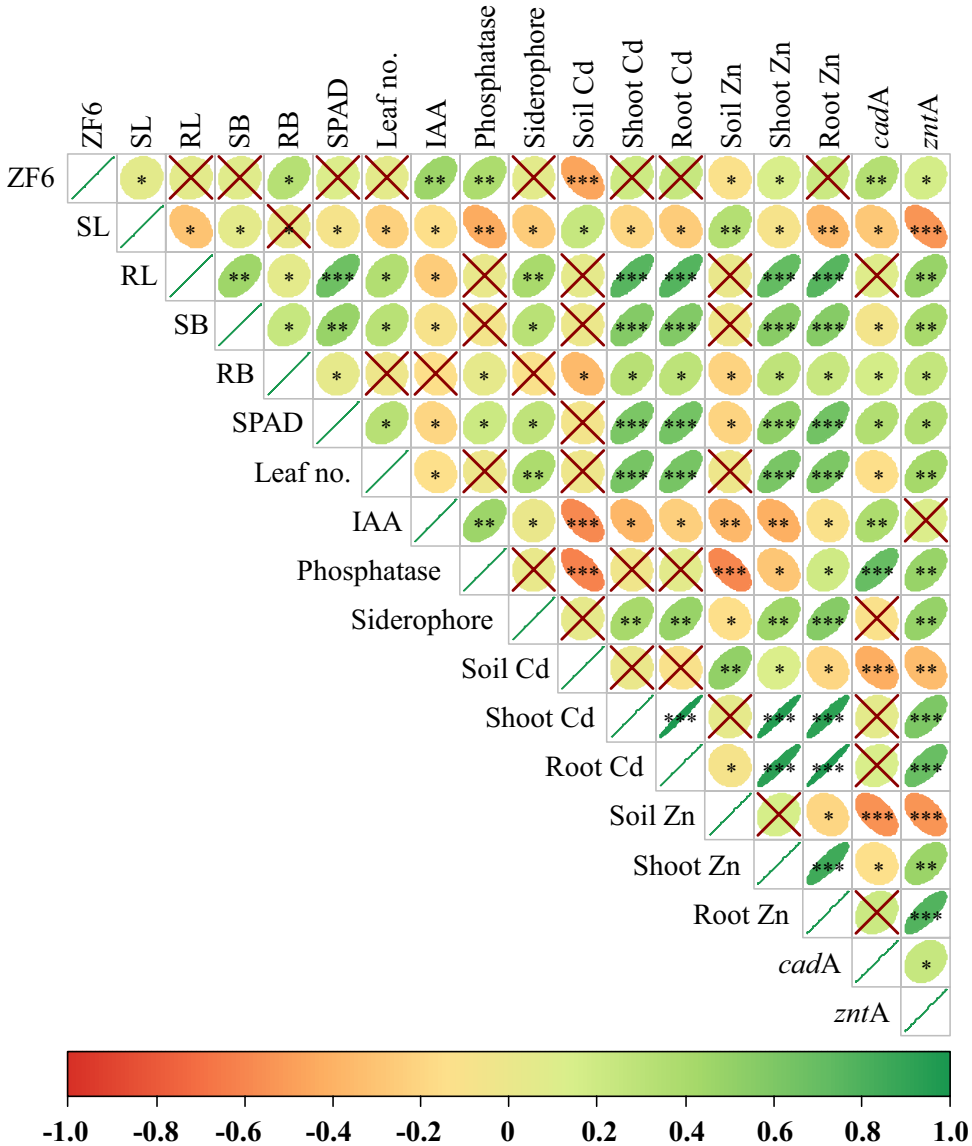


Fig. 1 Pearson correlation coefficient matrix of measured parameters, including plant growth factors, soil PGP activity, heavy metal concentrations, and heavy metal tolerance gene factors. *SL* shoot length, *RL* root length, *SB* shoot biomass, *RB* root biomass, *SPAD* SPAD value, *IAA* indole-3-acetic acid production, *Phosphatase* phosphatase activity, *Siderophore* siderophore production, *Soil Cd/Zn* Cd/Zn concentration in the tested soil, *Shoot Cd/Zn* Cd/Zn concentration in Chinese cabbage shoots, *Root Cd/Zn* Cd/Zn concentration in Chinese cabbage roots, *cad*A/*znt*A relative gene copy number of *cad*A and *znt*A in the tested soil. Asterisks (*) denote statistically significant correlations (*$p < 0.05$, **$p < 0.01$, ***$p < 0.001$). Green and red shading indicate positive and negative correlations, respectively

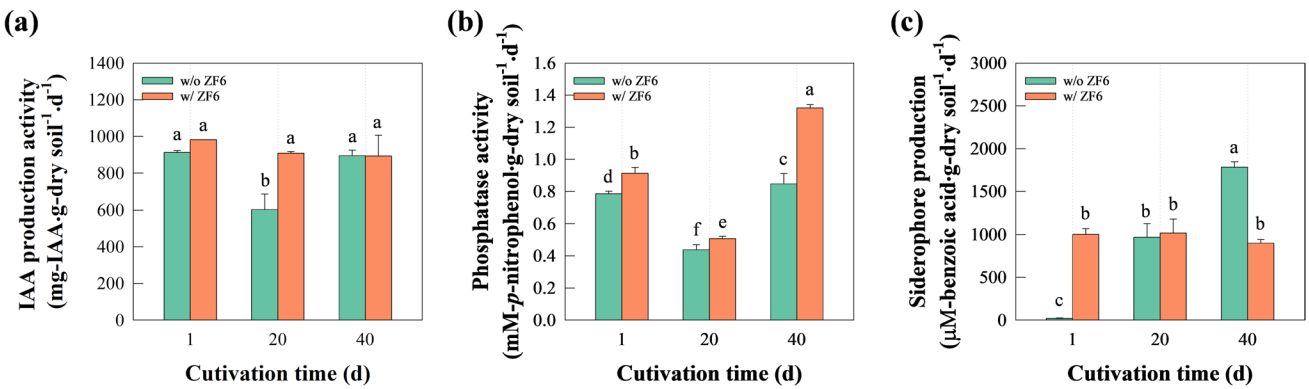


Fig. 2 Plant growth-promoting traits of *Burkholderia* sp. ZF6, including indole-3-acetic acid (IAA) production (**a**), phosphatase activity (**b**), and siderophore production (**c**). Treatments include w/o ZF6 (Chinese cabbage only) and w/ZF6 (Chinese cabbage with *Burkholderia* sp. ZF6). Each value represents the mean of triplicate data, with error bars indicating the standard deviation

contrast, siderophore production showed only transient differences and was not consistently enhanced by ZF6 inoculation (Fig. 2c). Correlation analysis of PGP traits indicated that IAA production ($r = 0.46$, $p = 0.001$) and phosphatase activity ($r = 0.38$, $p = 0.003$) were positively associated with ZF6 inoculation, whereas siderophore production showed no significant relationship.

The modest correlation coefficients observed (e.g., $r = 0.33$ for ZF6 inoculation vs. root biomass) align with typical ranges in ecological studies involving multifactorial systems. For instance, Muratova et al. 2023 reported comparable correlations ($r = 0.28$–0.69) between microbial inoculation and plant biomass in multi-metal-contaminated soils, attributing this to the complex interplay of abiotic and biotic factors. The statistical significance of these relationships ($p < 0.05$) despite their moderate strength underscores ZF6's measurable, albeit partial, role in shaping plant–microbe-metal dynamics. Overall, these results suggest that ZF6 inoculation selectively enhanced specific plant growth parameters and microbial functions, particularly root biomass and enzymatic activities, rather than uniformly affecting all growth indicators.

Effect of ZF6 inoculation on the removal of heavy metals from soil and their transfer to plants

The total concentrations of residual Cd and Zn in soil and plant tissues during phytoremediation of heavy metal-contaminated soils are presented in Fig. S5a and b. The absence of a consistent decrease in soil metal concentrations at day 20 relative to day 0 may be attributed to temporary fluctuations in metal availability and redistribution within the rhizosphere (Lee et al. 2024). In untreated Chinese cabbage (without ZF6 inoculation), the total soil Cd concentration significantly decreased to 60.8 mg·kg-soil^{-1} after 40 days compared to day 0, but the removal efficiency was only 5.1% (Fig. S5a). In contrast, ZF6-inoculated soil showed a greater reduction in Cd concentration, with a removal efficiency of 19.9%, indicating a substantially enhanced removal performance compared to the non-inoculated treatment. As shown in Fig. S5b, Zn concentration in soil increased after 20 days compared to the initial concentration, likely due to natural soil fluctuations (Śliwa-Cebula et al. 2020). Although Zn concentrations in ZF6-inoculated soil decreased slightly by day 40, this change was not statistically significant. Nevertheless, the removal efficiency (11.5%) was higher than that in the non-inoculated treatment, suggesting a potential contribution of ZF6 to Zn removal. Correlation analysis (Fig. 1) revealed a negative relationship between ZF6 inoculation and soil Cd concentration ($r = -0.46$), whereas the relationship with Zn was weak ($r = -0.11$).

Residual Cd and Zn concentrations in plant tissues are shown in Fig. S5c and d. ZF6 inoculation was associated with increased Cd accumulation in both shoots and roots, particularly at day 40 ($p < 0.05$). Similarly, Zn concentration in shoots was higher in the ZF6-inoculated group at day 20, whereas root Zn concentrations showed inconsistent trends between treatments over time (Fig. S5d). Correlation analysis indicated a generally weak relationship between ZF6 inoculation and metal accumulation in plant tissues, with most correlations not being statistically significant, except for Zn in shoots. Overall, these results suggest that ZF6 inoculation may enhance Cd removal and influence metal accumulation in plants, although the effects on Zn dynamics were more variable and less consistent.

Effect of ZF6 inoculation on the abundance of heavy metal resistance genes in soil

The temporal dynamics of *cad*A and *znt*A gene copy numbers revealed distinct patterns between ZF6-inoculated and non-inoculated soils during the 40-day phytoremediation

period (Fig. 3a and b). For *cad*A, both treatments started with similar gene copy numbers on day 1. In the non-inoculated treatment, the *cad*A copy number gradually declined, reaching about 40% of its initial value by day 40, suggesting a loss of Cd resistance potential in the absence of ZF6. In contrast, ZF6-inoculated soils exhibited a progressive increase in *cad*A copy number, culminating in a 2.7-fold higher value than the control at day 40 ($p < 0.05$). The *cad*A/16S rRNA ratio also remained stable or increased in the ZF6 treatment, indicating a sustained or enhanced proportion of Cd-resistant bacteria within the microbial community. For *znt*A, both treatments showed an overall increase in gene copy number over time, likely reflecting adaptation to persistent Zn stress. However, the increase was significantly pronounced in the ZF6-inoculated soils, where the *znt*A copy number was 1.2-fold higher than the control at day 40 ($p < 0.05$). Notably, the *znt*A/16S rRNA ratio in the ZF6 treatment rose more than fourfold by day 40, while it remained relatively unchanged in the non-inoculated group. These results indicate that ZF6 inoculation promoted the enrichment of heavy metal resistance genes in the rhizosphere, which may enhance soil Cd and Zn detoxification capacity and contribute to improved heavy metal removal and plant growth.

Effect of ZF6 inoculation on soil bacterial communities

Table 1 summarizes changes in amplicon sequence variants (ASVs) and alpha diversity (α-diversity) indices of bacterial communities in non-inoculated and ZF6-inoculated soils over time. In the non-inoculated treatment, both ASV counts and phylogenetic diversity (PD) tended to increase over time. In contrast, the ZF6-inoculated treatment showed the highest ASV and PD values on day 20, followed by a decline by day 40. The Shannon index also increased over time in the non-inoculated treatment, while the Gini–Simpson index remained relatively stable. In the ZF6-inoculated treatment, both the Shannon and Gini–Simpson indices exhibited a decreasing trend, indicating that bacterial community diversity increased in the non-inoculated treatment but declined in the ZF6-inoculated treatment over time. The composition of bacterial communities at the genus level, focusing on genera with relative abundances greater than 1%, is presented in Fig. 4a. *Rhodanobacter* was the dominant

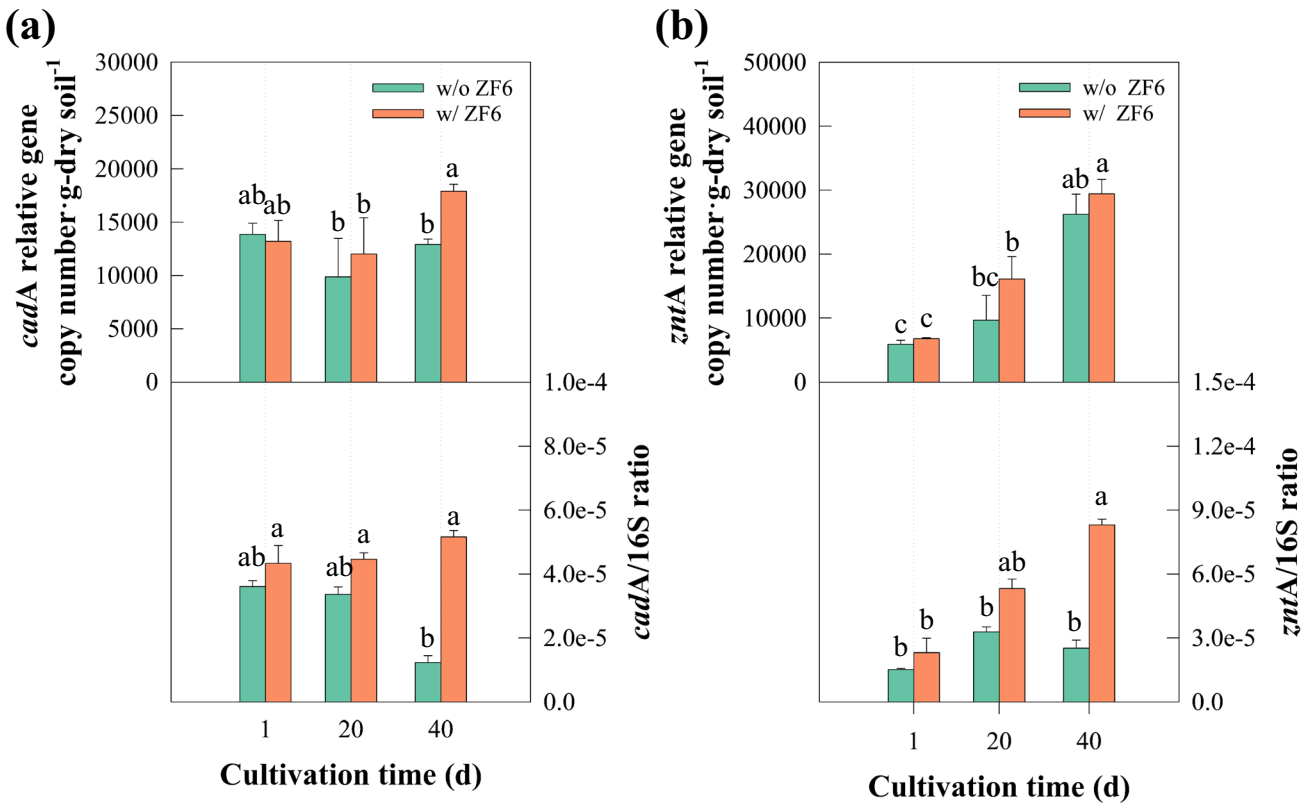


Fig. 3 Gene copy number of heavy metal tolerance genes in soil samples during the experimental period, showing *cad*A gene abundances (**a**) and *znt*A gene abundances (**b**). Treatments include w/o ZF6 (Chinese cabbage only) and w/ZF6 (Chinese cabbage with *Burkholderia* sp. ZF6). Each value represents the mean of triplicate data, with error bars indicating the standard deviation

Table 1 Amplicon sequence variants (ASVs) and alpha-diversity indices of the bacterial communities in the tested soils

Cultivation time (d)	Treatments	ASVs	Shannon[a]	Gini–Simpson[b]	Phylogenetic diversity[c]
1	w/o ZF6	638 ± 97	7.69 ± 0.14	0.99 ± 0.00	35.46 ± 5.14
	w/ZF6	719 ± 231	7.80 ± 0.16	0.99 ± 0.00	38.86 ± 9.45
20	w/o ZF6	797 ± 163	7.99 ± 0.11	0.99 ± 0.00	44.80 ± 4.52
	w/ZF6	954 ± 97	7.49 ± 0.12	0.98 ± 0.00	51.38 ± 5.25
40	w/o ZF6	823 ± 147	8.02 ± 0.11	0.99 ± 0.00	45.96 ± 4.46
	w/ZF6	679 ± 101	7.23 ± 0.13	0.97 ± 0.00	42.98 ± 2.85

[a]The Shannon index quantifies species diversity in a community

[b]The Gini–Simpson index measures species evenness, indicating how similar species abundances are across the community

[c]Phylogenetic diversity represents biodiversity based on evolutionary relationships, calculated as the sum of the branch lengths spanning all species in a community

genus across all treatments. In the non-inoculated treatment, the proportion of *Rhodanobacter* gradually declined, while *Sphingomonas*, *Reticulibacter*, and *Streptomyces* increased over time. In the ZF6-inoculated treatment, *Rhodanobacter* remained dominant until day 20, similar to day 1, but by day 40, *Pseudomonas* had become the most abundant genus. The heatmap in Fig. 4b shows clustering patterns of microbial communities and similarities among samples. On day 1, samples from both treatments exhibited similar microbial profiles. However, by days 20 and 40, distinct clustering patterns emerged between non-inoculated and inoculated treatments. The non-inoculated treatment was characterized by the presence of *Reticulibacter*, *Streptomyces*, *Sphingomonas*, *Bradyrhizobium*, and *Dyella*, while the ZF6-inoculated treatment showed higher abundances of *Klebsiella*, *Agrobacterium*, *Burkholderia*, *Sphingomonas*, and *Pseudomonas*. The PCA results, shown in Fig. 4c, further support these observations. In the non-inoculated treatment, bacterial communities on day 1 and day 20 displayed similar PCA patterns. In contrast, the ZF6-inoculated treatment showed increased cos2 values from day 20 to day 40, indicating a stronger correlation with the principal components and suggesting differences between the ZF6-inoculated treatments on days 20 and 40. This suggests that ZF6 inoculation increasingly influenced the structure of the soil bacterial community over time (Oliveira et al. 2024).

The VPA results identifying the primary factors influencing root-zone soil bacterial community structure are presented in Fig. 4d. ZF6 inoculation, heavy metal contamination, and soil plant growth-promoting enzyme activity (IAA, phosphatase, and siderophore) accounted for 13.9%, 29.6%, and 9.9% of the variation, respectively (Fig. 4d). Notably, the combination of just two variables, ZF6 inoculation effect and soil heavy metal contamination levels, explained 44.3% of the total 63.2%, highlighting them as the most influential factors shaping the microbial community structure. Only 5.2% of the variation was jointly explained by all variables, indicating a limited shared contribution across all factors.

To further explore ecological interactions among bacterial groups in both non-inoculated and ZF6-inoculated soils, a co-occurrence network analysis was conducted (Fig. 5). The resulting network structures differed significantly between treatments. The ZF6-inoculated network contained 282 nodes and 6599 edges—162 more nodes and 1462 more connections than the non-inoculated network (Table 2). Additionally, the average connectivity (avgK) was higher in the ZF6-inoculated treatment (46.80) compared to the non-inoculated treatment (18.05), indicating a more complex and interconnected microbial network. A similar trend was observed in the average clustering coefficient (Avg CC), which was also higher in the ZF6-inoculated treatment. Moreover, the average path distance (GD) was shorter in the ZF6-inoculated network (2.45) than in the non-inoculated one (2.55), suggesting higher transmission efficiency and closer connectivity among microbial taxa. In the non-inoculated treatment, *Sphingomonas* exhibited the highest number of connections and was identified as the key node in the network. In contrast, in the ZF6-inoculated treatment, *Pseudomonas*, *Klebsiella*, *Agrobacterium*, and *Burkholderia* were the most highly connected taxa and served as the primary hub nodes in the microbial network (Fig. 5). These shifts in microbial community composition may be associated with improved plant growth and enhanced heavy metal removal, suggesting a potential linkage between microbial community restructuring and soil–plant interactions under ZF6 inoculation.

Effect of ZF6 inoculation on the abundance of heavy metal resistance and transport-related functional genes in soil

The abundance of functional genes related to Cd and Zn resistance and transport was analyzed based on 16S rRNA gene-based functional predictions inferred using PICRUSt2 from contaminated soil samples (Fig. 6 and Table S2). These results represent predicted functional profiles rather

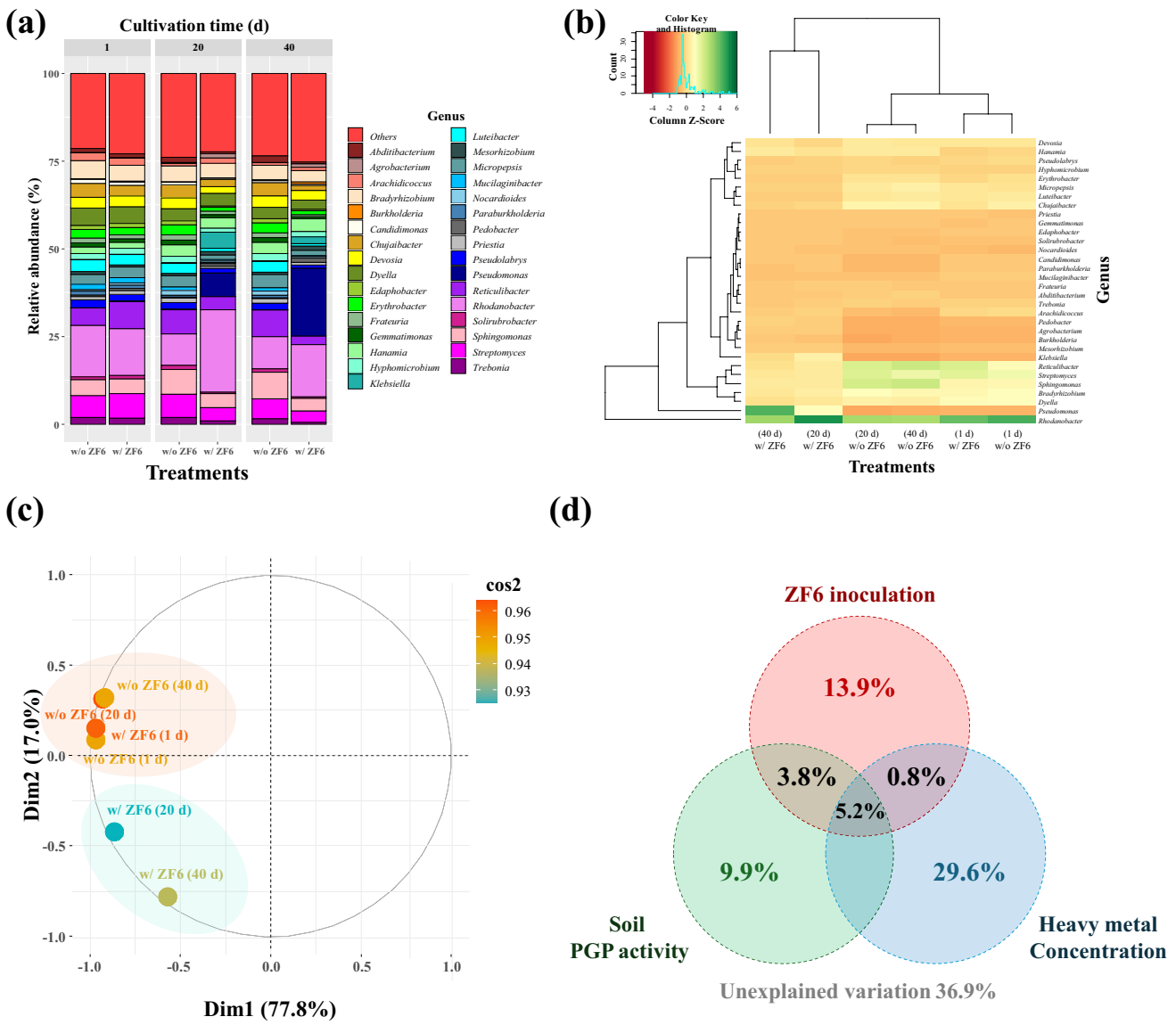


Fig. 4 Comparison of the bacterial community structure in the tested soil. **a** Relative bacterial community abundance on days 1, 20, and 40, with only genera having a total dominance of > 1% presented. **b** Hierarchically clustered heatmap of the bacterial distribution at the genus level, where rows represent bacterial genera, columns represent treatments, and relative abundance is indicated by color, increasing from red to green. **c** Principal component analysis (PCA) of the bacterial community structure in the soil, with cos2 values indicating each variable's contribution to principal components. Higher cos^2 values contribute more to the separation of data points. **d** Variation partitioning analysis (VPA) of the microbial community in tested soil, identifying four fractions: heavy metal contamination effect, soil PGP activity effect, ZF6 inoculation effect, and unexplained variation, with explained variance indicated by adjusted $r.^2$ values. Non-overlapping circles represent the percentage of variation explained by each factor alone, while overlapping regions represent shared contributions between factors (values < 0 not shown). Treatments include w/o ZF6 (Chinese cabbage only) and w/ZF6 (Chinese cabbage with *Burkholderia* sp. ZF6)

than direct measurements of gene expression. A total of 7117 KEGG orthologs (KOs) were identified across all soil samples. Notably, changes in the abundance of 10 representative genes associated with Cd and Zn resistance or transport, along with their correlations with rhizosphere bacterial communities, are presented in Fig. 6. Over time, the abundance of all 10 functional genes in the ZF6-inoculated treatment showed an increasing trend compared to the non-inoculated treatment (Fig. 6a and Table S2). Particularly, the H8 (K01915) gene, involved in glutamine synthesis and playing a key role in nitrogen metabolism, while also serving as a stress indicator under Cd exposure, was the most abundant among the 10 functional genes (28%), and its abundance increased by 1.6 times compared to the non-inoculated treatment. Additionally, the H3 (K01534) gene, which is associated with Cd and Zn resistance and transport

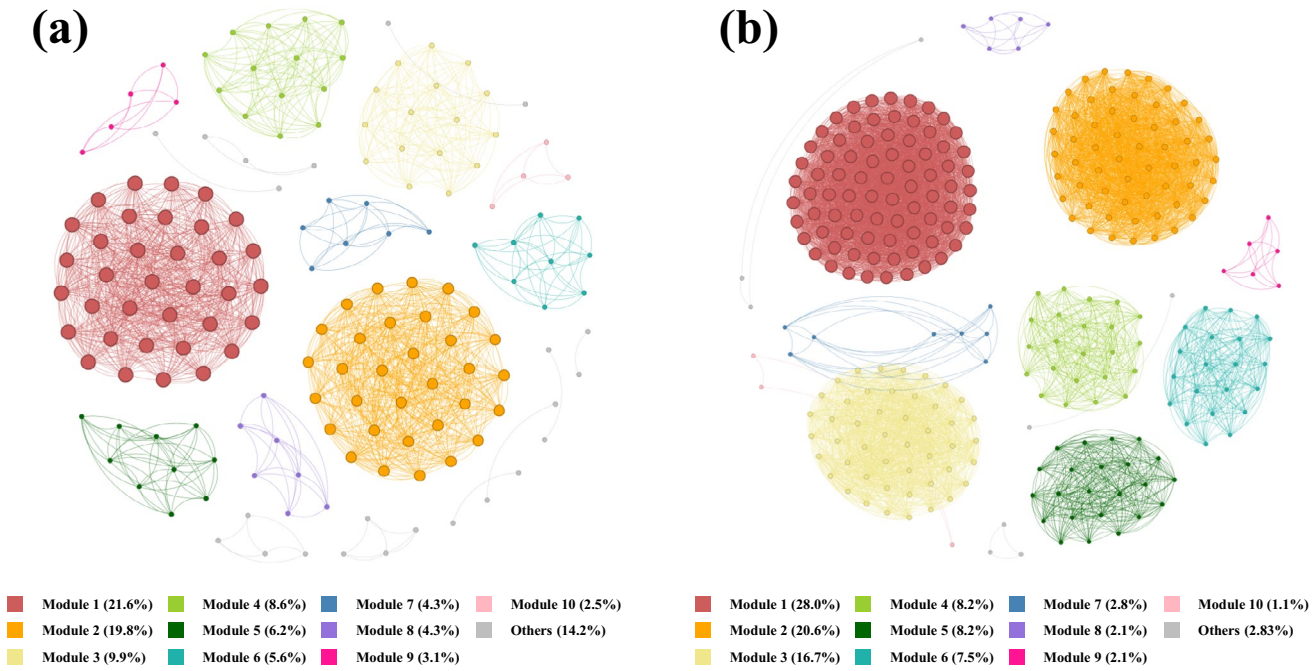


Fig. 5 Microbial modular analysis of the bacterial communities in tested soils without ZF6 (**a**) and with ZF6 (**b**). The size of each node is proportional to the connectivity of the operational taxonomic unit (OTU), and different colors represent distinct modules within the networks. Only genera with a total dominance of > 1% are presented. Treatments include w/o ZF6 (Chinese cabbage only) and w/ZF6 (Chinese cabbage with *Burkholderia* sp. ZF6)

(i.e., *znt*A), increased by more than twofold, while the H4 (K07238) gene, which is associated with metal ion transport, increased by approximately 1.9-fold. Three other genes—H2 (K01533), H5 (K03781), which are associated with Cd and Zn resistance, and H7 (K02016), which is associated with Cd transport, all exhibited abundances exceeding 10% (Fig. 6a). The K01533 and K01915 genes showed positive correlations with *Mesorhizobium* and *Pedobacter* ($p < 0.05$), and negative correlations with *Micropepsis*, *Hyphomicrobium*, and *Abditibacterium* (Fig. 6b). The K01534 gene was positively correlated with *Agrobacterium*, *Pseudomonas*, and *Burkholderia*, but negatively correlated with *Streptomyces*, *Devosia*, *Luteibacter*, and *Bradyrhizobium*. The K07238 gene showed positive correlations with *Agrobacterium* and *Pseudomonas*, while the H6 (K02010) gene, which is associated with Zn transport, was positively correlated with *Rhodanobacter, Pedobacter*, and *Burkholderia*.

Table 2 Topological properties of the soil bacterial community molecular ecological networks under tested soils

Network indices	w/o ZF6[d]	w/ ZF6
Cutoff	0.40	0.40
Nodes	162	282
Edges	1462	6599
Avg K[a]	18.05	46.80
Avg CC[b]	0.11	0.17
GD[c]	2.55	2.45
Modularity	0.71	0.69
Modules	19	13

[a]Average degree (*K*): The number of edges connected to a node in the network

[b]Average clustering coefficient (*CC*): The overall tendency of nodes in a network to form tightly connected groups

[c]Average path distance (*Graph density*): The average shortest path between all pairs of nodes in the network

[d]*w/o ZF6* Chinese cabbage only, *w/ ZF6* Chinese cabbage + *Burkholderia* sp. ZF6

Additionally, correlation analysis between the 10 functional genes and heavy metal-related factors revealed that the abundance of the *znt*A gene in rhizosphere soil had strong positive correlations with the H1 (K04565) gene, which is associated with the removal of reactive oxygen species (ROS) generated under Cd and Zn stress, as well as with the K01534 gene (Fig. 6b). The accumulation of Cd and Zn in the shoots and roots of Chinese cabbage was positively correlated with the K04565, K01534, and K07238 genes. In contrast, total Cd content in the rhizosphere soil showed negative correlations with the K01533 and K02010 genes. Overall, these results indicate that ZF6 inoculation may influence the predicted functional potential of the soil microbial community; however, these interpretations should

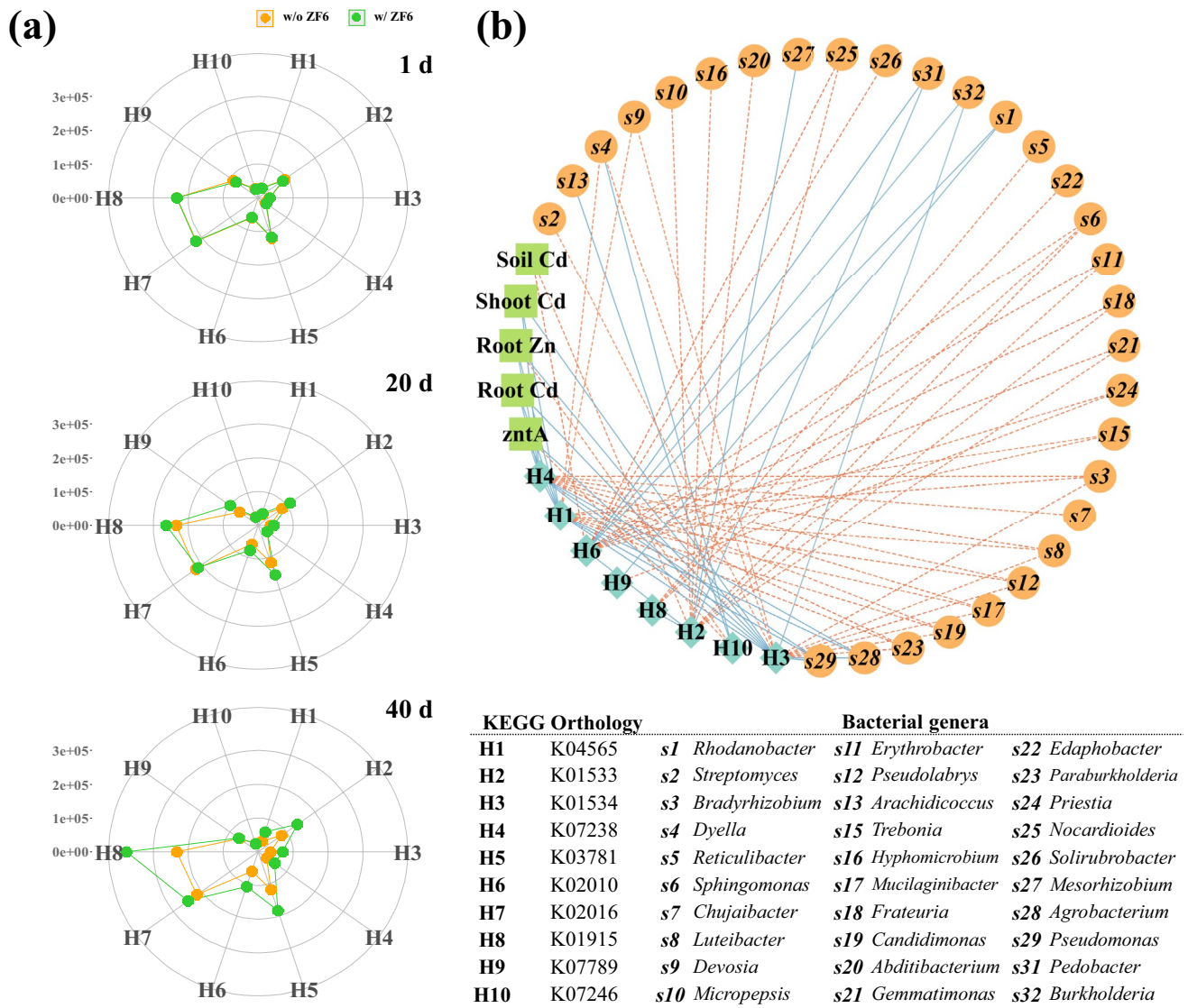


Fig. 6 **a** Radar plots showing the distribution of functional genes involved in heavy metal metabolism between Kyoto Encyclopedia of Genes and Genomes (KEGG) ortholog (KO) groups in tested soils without ZF6 (orange) and with ZF6 (green) over 40 days. Treatments include w/o ZF6 (Chinese cabbage only) and w/ZF6 (Chinese cabbage with *Burkholderia* sp. ZF6). **b** Association network analysis between heavy metal concentration factors and bacterial genera. *Soil Cd* Cd concentration in the tested soil, *Shoot Cd* Cd concentration in the Chinese cabbage shoot, *Root Cd/Zn* Cd/Zn concentration in the Chinese cabbage root, *znt*A relative gene copy number of *znt*A in the tested soil. Solid blue and dashed red edges indicate significant positive and negative relationships, respectively ($p < 0.05$)

be considered indicative trends rather than direct evidence of gene activity or metabolic processes.

Discussion

PGP effects

The increase in PGP activity in soil not only supports plant development but also enhances resistance to metal stress, thereby providing protection for crops (Wang et al. 2022). In this study, ZF6 inoculation increased soil PGP activity, contributing to plant growth (Figs. 1, 2, and S4). ZF6 exhibited strong nitrogen-fixing ability, along with the production of IAA and phosphorus solubilization capacity (Lee and Cho 2025), which resulted in increased IAA levels and phosphatase activity in the rhizosphere soil of Chinese cabbage (Fig. 2a and b). These changes suggest that even under toxic Cd and Zn stress, root biomass and chlorophyll content in Chinese cabbage increased (Fig. S4b and c). This finding aligns with previous reports that bacteria belonging to the same genus as ZF6, including *B. cepacia, B. gladioli*, and *B. graminis*, possess IAA production and phosphate solubilization capabilities, promoting root and shoot growth (dos

Santos et al. 2021; Li et al. 2022). Bacterial IAA acts as a phytohormone that influences root development (Mohite 2013; Ganesh et al. 2024), while phosphatase activity converts organic phosphate into plant-available forms, improving nutrient uptake under metal stress (Campdelacreu Rocabruna et al. 2024). Together, IAA production and phosphatase activity likely contributed to reduced metal stress and enhanced nutrient acquisition, supporting the growth of Chinese cabbage (Fig. S4). These findings are consistent with previous studies reporting that PGPB, including *Burkholderia* sp., enhance plant growth under heavy metal stress through phytohormone production and nutrient mobilization, although the magnitude of growth promotion observed in this study suggests that ZF6 may possess enhanced multifunctional capabilities.

While ZF6 exhibits siderophore production in vitro (Fig. S1 and Table S1), its inoculation did not increase net soil siderophore activity (Fig. 2c). This apparent contradiction arises from two factors. Cd/Zn levels (71.8 mg-Cd·kg-soil^{-1}, 1683 mg-Zn·kg-soil^{-1}) suppressed siderophore synthesis across the microbial community, including ZF6. For instance, 50 mg-Cd·kg-soil^{-1} has been shown to reduce siderophore production in *Pseudomonas fluorescens* by 40–60% (Balta et al. 2025). Additionally, ZF6's siderophores may have been preferentially utilized by itself or neighboring taxa under metal stress, limiting detectability in soil assays (Liu et al. 2024a; Syed et al. 2023). Notably, the negative correlation suggests heavy metal stress favors metal-resistant microbes over siderophore producers. (Huo et al. 2021; Liu et al. 2024a). While ZF6 maintains baseline siderophore production (Fig. S2), its contribution was likely overshadowed by HM-induced suppression of siderophore synthesis in sensitive indigenous microbes (Wu et al. 2021). This highlights the complex interplay between HM toxicity and microbial metabolic trade-offs in contaminated soils (Lear et al. 2023; Liu et al. 2024a).

Heavy metal removal effect

ZF6 inoculation significantly improved the removal efficiency of Cd and Zn from the soil, achieving rates approximately 2 to 4 times higher than those observed in the non-inoculated treatment (Fig. S5a and b). The higher Cd removal efficiency (19.9%) compared to Zn (11.5%) may be attributed to differences in plant physiological requirements and metal transport behavior (Balafrej et al. 2020; Chen 2023). Zn, as an essential micronutrient, is tightly regulated through uptake systems, whereas Cd, a non-essential metal, is more readily accumulated due to less selective transport (Balafrej et al. 2020; Chen 2023). This trend is consistent with previous findings in *Brassica juncea*, where Cd uptake exceeded Zn under co-contamination conditions (Balafrej et al. 2020). Additionally, ZF6's *cad*A/*znt*A efflux systems may contribute to increased Cd availability in the rhizosphere, thereby enhancing phytoextraction (Liu et al. 2024a; Singh et al. 2016), whereas Zn dynamics may be partially regulated by plant uptake mechanisms (Liu et al. 2024a; Singh et al. 2016). Recent studies also report stronger associations between *cad*A expression and Cd removal than between *znt*A and Zn (Liu et al. 2024a).

The enhanced removal efficiency may also be related to multiple microbial mechanisms, including metal efflux, biosorption, intracellular accumulation, and plant growth promotion. PGPB such as ZF6 can increase metal bioavailability, adsorb metals through cell surface functional groups, and enhance plant growth via phytohormone production and nutrient solubilization (Wang et al. 2022; Liu et al. 2024b; Qin et al. 2024; Gogoi et al. 2024). These processes collectively contribute to increased plant biomass and metal uptake capacity (Gogoi et al. 2024). As shown in Fig. 1, the negative correlation between ZF6 inoculation and soil metal content suggests that ZF6 contributes to the reduction of heavy metals in the soil. Although the contamination levels in this study were relatively high, which may suppress indigenous microbial activity (Gamalero and Glick 2024), ZF6 inoculation still enhanced Cd and Zn removal. Given that phytoremediation generally requires extended timeframes (Gamalero and Glick 2024), further long-term studies are needed.

The effectiveness of phytoremediation largely depends on plant biomass and metal uptake capacity (Wang et al. 2021). Chinese cabbage, particularly species within the *Brassica* genus, is considered suitable for phytoextraction due to its high biomass production and metal accumulation ability (Wang et al. 2021; Liao et al. 2023). In this study, ZF6 inoculation enhanced Zn uptake in shoots (Figs. S4 and S5d), suggesting that ZF6 contributed to improved plant growth and metal translocation. Zn, an essential micronutrient, is generally more readily transported within plants than Cd (Hamzah Saleem et al. 2022; Chen 2023). Thus, the combined effects of plant characteristics and ZF6 inoculation likely contributed to enhanced metal uptake and removal (Bortoloti and Baron 2022). This observation is in agreement with previous reports showing that PGPB can enhance metal uptake and removal efficiency by altering metal bioavailability and plant physiological responses, indicating that ZF6 functions within similar mechanisms under Cd and Zn stress conditions.

Increase in heavy metal resistance genes in soil

The *cad*A and *znt*A genes encode P-type ATPases that are associated with resistance to Cd and Zn by exhibiting high binding affinity to these ions, thereby contributing to the mitigation of metal toxicity (Lu et al. 2016; Prabhakaran and Thamarai 2024). The *cad*A gene is particularly

effective at binding and exporting Cd ions, which may reduce cellular damage and contribute to Cd detoxification in the surrounding environment (Prabhakaran and Thamarai 2024). In contrast, *znt*A exhibits strong affinity for both Cd and Zn and is associated with the regulation of metal ion mobility in soil, potentially enhancing the efficiency of phytoremediation (Lu et al. 2016). Notably, *znt*A is induced under high Zn concentrations and has been reported to be involved in Zn regulation through plant–microbe interactions (Lu et al. 2016).

In this study, the abundance of both genes in the rhizosphere soil of Chinese cabbage showed a positive correlation with ZF6 inoculation (Figs. 1 and 3). While total bacterial abundance (16S rRNA gene copy number) did not differ significantly at the initial stage, it increased markedly in the ZF6-inoculated treatment by day 40 compared to the non-inoculated treatment (Fig. 3a). Moreover, the *cad*A/16S and *znt*A/16S gene ratios also increased with ZF6 inoculation (Fig. 3), indicating an enrichment of Cd- and Zn-resistant bacteria within the microbial community (González Henao and Ghneim-Herrera 2021). The presence of these metal-resistant bacteria reflects adaptation to heavy metal stress and may contribute to enhanced phytoremediation performance (González Henao and Ghneim-Herrera 2021). Specifically, the inoculation of ZF6, which harbors both *cad*A and *znt*A genes, may have contributed to an increased metal resistance potential of the soil microbiome. This may be associated with reduced metal toxicity in plants, thereby promoting plant growth (Figs. 1, 3, and S4). Consistent with previous studies, microbial inoculation in contaminated soils has been shown to increase the abundance of heavy metal resistance genes and associated functional traits, suggesting that microbial communities may adapt to metal stress through the selective enrichment of genes involved in metal efflux, detoxification, and homeostasis (Li et al. 2023; Sun et al. 2025).

In addition, further in-depth studies, such as additional metatranscriptomics analyses, are needed in the future to obtain direct evidence for the role of *cad*A/*znt*A in Cd/Zn removal. Therefore, the relationship observed in this study should be interpreted as a correlation rather than direct mechanistic evidence. For example, a *cad*A-deficient *Burkholderia cepacia* showed a 70% decrease in Cd efflux ability, suggesting its critical role in metal detoxification (Schwager et al. 2012). Recent studies in *Pseudomonas putida* further confirm that *cad*A homologs are essential for Cd resistance, with knockout mutants exhibiting severe growth defects under Cd stress (Royet et al. 2025). While direct knockout validation was beyond this study's scope, the correlation between *cad*A/*znt*A abundance and metal removal is consistent with previous mechanistic studies in *Burkholderia cepacia* and *Pseudomonas putida*.

Impact on soil bacterial communities

To better understand rhizosphere microbial dynamics, this study examined the effects of ZF6 inoculation, which was associated with a more complex microbial network and increased core genera (Figs. 4, 5, and 6). Key genera, including *Pseudomonas, Klebsiella, Agrobacterium*, and *Burkholderia*, were predominant in ZF6-inoculated treatments (Fig. 4). Tree-map analysis showed that these genera belonged to Pseudomonadota, Gemmatimonadota, and Actinomycetota, which became dominant after ZF6 inoculation (Fig. S6). Bacteria from Pseudomonadota are widely reported in heavy metal-contaminated environments, while Gemmatimonadota has been associated with Zn resistance (Yu et al. 2021; Li et al. 2025; Hu et al. 2021). The enrichment of *Pseudomonas* and *Klebsiella* (Fig. 4a) is consistent with their reported roles in metal resistance and plant–microbe interactions. Genomic analyses indicate that *Pseudomonas* can harbor *cad*A and *znt*A homologs involved in Cd^{2+}/Zn^{2+} efflux, and can contribute to metal sequestration through extracellular polymeric substances (Ducret et al. 2020, 2021; Prabhakaran and Thamarai 2024; Chatterjee et al. 2024). Similarly, *Klebsiella* was identified as a significant biomarker in the ZF6 treatment (Fig. S7), and its metal resistance has been associated with efflux systems and siderophore production (Kusale et al. 2021; Balta et al. 2025). The co-enrichment of these genera with ZF6 suggests a potential functional association under metal stress. Overall, ZF6 inoculation, together with environmental selection pressure, may contribute to the enrichment of metal-resistant bacteria in the rhizosphere of Chinese cabbage (Figs. S6 and S7). Additionally, these microbial shifts are consistent with previous studies indicating that inoculation with PGPB can restructure native microbial communities toward metal-resistant and plant-beneficial taxa, thereby influencing soil–plant interactions under contaminated conditions (Ducret et al. 2020, 2021; Kusale et al. 2021; Chatterjee et al. 2024; Prabhakaran and Thamarai 2024).

Alpha-diversity analysis (Table 1) revealed that ZF6 inoculation reduced microbial diversity compared to the non-inoculated treatment. This suggests that a smaller number of metal-adapted taxa, including Pseudomonadota and *Klebsiella*, became dominant. The decrease in diversity (Table 1), despite increased heavy metal resistance genes (Figs. 3 and 6), may be explained by environmental filtering and functional specialization (Wang et al. 2023). ZF6-associated taxa (e.g., *Pseudomonas, Klebsiella*, and *Burkholderia*) likely outcompeted less resistant species, reducing diversity (Liu et al. 2022; Wang et al. 2023). Network analysis showed higher connectivity and modularity in ZF6-inoculated soils (Fig. 5, Table 2), indicating stronger interactions among specialized taxa (Chen et al. 2022). These patterns may also be associated with adaptive processes such as horizontal gene

transfer (HGT) (Balta et al. 2025). *Klebsiella* species are known for heavy metal resistance and plant growth-promoting traits (Kusale et al. 2021; Kim et al. 2022), and *Burkholderia* increased in abundance over time (Figs. 4a and S6). This coincided with improved metal removal and root biomass (Figs. S4 and S5), suggesting a link between microbial shifts and plant performance. However, it should be noted that soil heat sterilization likely altered the native microbial community structure, which may limit the direct ecological interpretation of the results. Therefore, the observed microbial dynamics primarily reflect responses under controlled conditions rather than fully representing natural soil ecosystems. Further studies under non-sterilized and field conditions are required to validate these findings.

Impact on the abundance of functional genes related to heavy metal resistance in soil

Bacteria inhabiting the plant rhizosphere are known to carry various genes, such as *cad*A, *cad*B, *chr*A, *pbr*A, *Mer*A, *znt*A, and NiCoT, associated with resistance, detoxification, and transport mechanisms for heavy metals (Nnaji et al. 2024). In this study, the distribution of Cd- and Zn-related functional genes was analyzed in contaminated soil samples (Fig. 6 and Table S2). These analyses are based on inferred functional profiles derived from 16S rRNA gene data and should not be interpreted as direct measurements of gene expression. Among them, the K04565 gene, associated with scavenging ROS generated under Cd and Zn stress, showed a positive correlation with both *znt*A abundance in the rhizosphere and metal accumulation in Chinese cabbage (Fig. 6b). K04565 has been reported to mitigate cellular damage by eliminating ROS under metal toxicity conditions (Zhou et al. 2022). Previous research has also demonstrated its role in protecting plants and microbes from oxidative stress in Pb-contaminated environments (Zhang et al. 2023a).

The K01534 gene, associated with Cd and Zn resistance and transport, showed more than a twofold increase in abundance following ZF6 inoculation compared to the non-inoculated treatment (Fig. 6a). Notably, K01534 positively correlated with the genera *Agrobacterium*, *Pseudomonas*, and *Burkholderia* (the latter corresponding to ZF6). This gene, also known as *znt*A, encodes a P-type ATPase involved in the export of Cd and Zn from the cell (Rensing et al. 1997; Wang et al. 2024). By regulating intracellular metal ion concentrations, K01534 may contribute to reduced cellular damage and adaptation to heavy metal stress. The presence of ZF6, which harbors *znt*A, may have contributed to the increase in K01534 over time (Fig. 6a), which may be associated with enhanced metal accumulation in Chinese cabbage (Fig. 6b). ZF6's *znt*A is known to encode a P-type ATPase that exports Zn^{2+}/Cd^{2+} via ATP hydrolysis (Fakhar et al. 2022), and similar efflux activity has been suggested to reduce intracellular metal toxicity and facilitate plant uptake (Ducret et al. 2020). The negative correlation between K01534 abundance and soil Cd content (Fig. 6b) is consistent with these reported functions (Zhu et al. 2025). Similarly, earlier studies reported that functional metal-resistance genes became dominant after short-term cultivation in contaminated soils, corresponding with shifts in dominant bacterial genera (Yang et al. 2024). In addition, *Bacillus megaterium* HgT21, which harbors the *znt*A gene, has been shown to confer multi-metal resistance and promote plant growth under metal stress (Guzmán-Moreno et al. 2022).

The H4 (K07238) gene, involved in metal ion transport, showed an approximately twofold increase in abundance following ZF6 inoculation compared to the non-inoculated treatment (Fig. 6a). K07238 encodes Zn transporter proteins of the ZIP family, which regulate intracellular Zn levels and facilitate metal transport in plants (Gilbert et al. 2025). The K07238 gene, homologous to *Brassica* ZIP2/ZIP4 transporters, has been reported to facilitate Zn^{2+}/Cd^{2+} influx into root cells (Zhang et al. 2023b), and structural studies indicate that these transporters preferentially bind Zn^{2+} but can also transport Cd^{2+} (Ajeesh Krishna et al. 2020). This may explain the positive correlation between K07238 abundance and Cd accumulation in shoots (Fig. 6b). Our results suggest that ZF6 inoculation, together with native bacteria such as *Agrobacterium* and *Pseudomonas*, may be associated with enhanced metal transport from soil to plants, supported by the observed correlation between K07238 and Zn accumulation in Chinese cabbage (Fig. 6b). Similarly, previous studies have reported that inoculation with metal-resistant *Bacillus* sp. is associated with increased abundance of genes related to metal transport and detoxification, including the ABC, HMA, ZIP, and MTP families, thereby enhancing phytoremediation potential (Liu et al. 2024a).

The H6 (K02010) gene, which is indirectly involved in Zn transport, was positively correlated with dominant bacterial genera observed in this study, including *Rhodanobacter*, *Pedobacter*, and *Burkholderia* (Fig. 6b). K02010 has been reported to be associated with iron transport and may contribute to the supply of trace metals such as Zn as essential micronutrients (Galisteo et al. 2023). It has also been linked to osmotic balance and heavy metal resistance in contaminated soils (Galisteo et al. 2023). In this study, the increased abundance of bacterial genera associated with K02010 may be linked to enhanced metal resistance and plant growth (Figs. 1, 6, and S4). However, it should be noted that these functional predictions are based on inferred gene profiles rather than direct measurements, and therefore should be interpreted as potential functional trends rather than confirmed metabolic activities.

The high abundance of heavy metal resistance genes observed in the metagenomic analysis may be attributed to the elevated levels of Cd and Zn already present in the soil,

as well as the existence of soil microorganisms, such as ZF6, which possess genetic systems for resistance and transport to mitigate metal toxicity (Phurailatpam et al. 2022). These findings suggest that ZF6 inoculation may have influenced the rhizosphere bacterial community, thereby influencing the composition and abundance of functional genes related to Cd and Zn resistance and transport (Fig. 6). Our results are consistent with previous reports demonstrating that inoculation with metal-resistant bacteria can enhance plant growth and metal uptake while increasing the abundance of resistance genes in the soil microbiome. For instance, Liu et al. (2024a, b) reported that *Bacillus* sp. inoculation in *Sedum alfredii* facilitated heavy metal phytoextraction and upregulated resistance genes. However, our study extends these findings by showing that *Burkholderia* sp. ZF6 not only increases Cd/Zn removal and plant biomass but also is associated with increases in microbial network complexity and the abundance of multiple resistance genes (*cad*A, *znt*A, K01534, and K07238) (Khatoon et al. 2024). This may indicate a broader effect on rhizosphere microbial interactions, which has not been fully addressed in previous studies. In addition, the relatively short experimental duration (40 days) may limit the assessment of long-term effects of ZF6 inoculation on soil microbial dynamics and plant–microbe interactions.

Conclusion

This study examined the effects of *Burkholderia* sp. ZF6, a PGPB with heavy metal resistance genes, on plant growth and heavy metal removal in Cd- and Zn-contaminated soils. ZF6 enhanced soil enzyme activities, including IAA production and phosphatase activity, which contributed to increased root biomass and length in Chinese cabbage. Additionally, ZF6 facilitated heavy metal uptake by plants, thereby reducing soil Cd and Zn concentrations. Inoculation with ZF6 also altered the composition and functional potential of bacterial communities in contaminated soils, promoting the proliferation of *Agrobacterium*, *Burkholderia*, *Sphingomonas*, and *Pseudomonas*. These shifts in the rhizosphere microbiome were associated with an increased abundance of heavy metal resistance and transport-related genes (K01915, K01534, and K07238), based on predictive functional profiling. The findings provide insights into the potential role of ZF6 in shaping microbial communities and enhancing heavy metal resistance-related functional potential in contaminated soils. However, this study was conducted under controlled pot conditions over a relatively short duration (40 days), and the functional gene analysis was based on predictive approaches. Therefore, the broader applicability and mechanistic interpretations should be considered with caution. Future research should focus on validating the effectiveness of ZF6 under field-scale conditions and assessing its long-term ecological impacts, including its interactions with native soil microbial communities across varying contamination levels and the regulatory mechanisms underlying heavy metal resistance gene expression.

Supplementary Information The online version contains supplementary material available at https://doi.org/10.1007/s11356-026-37770-4.

Author contribution Soo Yeon Lee and Kyung-Suk Cho contributed to the study conception and design. Material preparation and data collection were performed by Soo Yeon Lee. Data analysis was performed by Soo Yeon Lee and Kyung Suk Cho. The first draft of the manuscript was written by Soo Yeon Lee, and Kyung Suk Cho commented on the previous version of the manuscript. All the authors read and approved the final manuscript.

Funding Open Access funding enabled and organized by Ewha Womans University. This work was supported by the National Research Foundation of Korea (NRF) grant, funded by the Korean government (Ministry of Science and ICT [MSIT]) (No. 2022R1A2C2006615), and by the Particulate Matter Management Specialized Graduate Program through the Korea Environmental Industry & Technology Institute (KEITI), funded by the Ministry of Environment (MOE).

Data availability The data supporting the findings of this study are available within the article and its supplementary materials.

Declarations

Ethical approval This research does not involve human or animal subjects, therefore, ethical approval was not required.

Consent to participate This study did not involve human participants, and consent to participate was not applicable.

Consent for publication This study did not involve human participants, and consent for publication was not applicable.

Competing interests The authors declare no competing interests.

Open Access This article is licensed under a Creative Commons Attribution-NonCommercial-NoDerivatives 4.0 International License, which permits any non-commercial use, sharing, distribution and reproduction in any medium or format, as long as you give appropriate credit to the original author(s) and the source, provide a link to the Creative Commons licence, and indicate if you modified the licensed material. You do not have permission under this licence to share adapted material derived from this article or parts of it. The images or other third party material in this article are included in the article's Creative Commons licence, unless indicated otherwise in a credit line to the material. If material is not included in the article's Creative Commons licence and your intended use is not permitted by statutory regulation or exceeds the permitted use, you will need to obtain permission directly from the copyright holder. To view a copy of this licence, visit http://creativecommons.org/licenses/by-nc-nd/4.0/.

References

Ajeesh Krishna TP, Maharajan T, Victor Roch G, Ignacimuthu S, Antony Ceasar S (2020) Structure, function, regulation and

phylogenetic relationship of ZIP family transporters of plants. Front Plant Sci 11:662. https://doi.org/10.3389/fpls.2020.00662

Ajmal AW, Yasmin H, Hassan MN, Khan N, Jan BL, Mumtaz S (2022) Heavy metal–resistant plant growth–promoting *Citrobacter werkmanii* strain WWN1 and *Enterobacter cloacae* strain JWM6 enhance wheat (*Triticum aestivum* L.) growth by modulating physiological attributes and some key antioxidants under multi-metal stress. Front Microbiol 13:815704. https://doi.org/10.3389/fmicb.2022.815704

Balafrej H, Bogusz D, El Abidine Triqui Z, Guedira A, Bendaou N, Smouni A, Fahr M (2020) Zinc hyperaccumulation in plants: a review. Plants 9:562. https://doi.org/10.3390/plants9050562

Balta I, Lemon J, Gadaj A, Cretescu I, Stef D, Pet I, Stef L, McCleery D, Douglas A, Corcionivoschi N (2025) The interplay between antimicrobial resistance, heavy metal pollution, and the role of microplastics. Front Microbiol 16:1550587. https://doi.org/10.3389/fmicb.2025.1550587

Bazzi W, Abou Fayad AG, Nasser A, Haraoui L-P, Dewachi O, Abou-Sitta G, Nguyen V-K, Abara A, Karah N, Landecker H, Knapp C, McEvoy MM, Zaman MH, Higgins PG, Matar GM (2020) Heavy metal toxicity in armed conflicts potentiates AMR in *A. baumannii* by selecting for antibiotic and heavy metal co-resistance mechanisms. Front Microbiol 11:68. https://doi.org/10.3389/fmicb.2020.00068

Benitez E, Melgar R, Nogales R (2004) Estimating soil resilience to a toxic organic waste by measuring enzyme activities. Soil Biol Biochem 36:1615–1623. https://doi.org/10.1016/j.soilbio.2004.07.014

Bortoloti GA, Baron D (2022) Phytoremediation of toxic heavy metals by *Brassica* plants: a biochemical and physiological approach. Environ Adv 8:100204. https://doi.org/10.1016/j.envadv.2022.100204

Campdelacreu Rocabruna P, Domene X, Preece C, Peñuelas J (2024) Relationship among soil biophysicochemical properties, agricultural practices and climate factors influencing soil phosphatase activity in agricultural land. Agriculture 14:288. https://doi.org/10.3390/agriculture14020288

Chatterjee S, Barman P, Barman C, Majumdar S, Chakraborty R (2024) Multimodal cadmium resistance and its regulatory networking in Pseudomonas aeruginosa strain CD3. Sci Rep 14:31689. https://doi.org/10.1038/s41598-024-80754-y

Chen S (2023) Mechanism of Zn alleviates Cd toxicity in mangrove plants (*Kandelia obovata*). Front Plant Sci 13:1035836. https://doi.org/10.3389/fpls.2022.1035836

Chen H, Ma K, Lu C, Fu Q, Qiu Y, Zhao J, Huang Y, Yang Y, Schadt CW, Chen H (2022) Functional redundancy in soil microbial community based on metagenomics across the globe. Front Microbiol 13:878978. https://doi.org/10.3389/fmicb.2022.878978

Chen E, Yang C, Tao W, Li S (2024) Polysaccharides produced by plant growth-promoting rhizobacteria strain Burkholderia sp. BK01 enhance salt stress tolerance to Arabidopsis thaliana. polymers (basel) 16:145. https://doi.org/10.3390/polym16010145

Dobrzyński J, Kulkova I, Jakubowska Z, Wróbel B (2025) Non-native PGPB consortium consisting of Pseudomonas sp. G31 and Azotobacter sp. PBC2 promoted winter wheat growth and slightly altered the native bacterial community. Sci Rep 15:3248. https://doi.org/10.1038/s41598-025-86820-3

dos Santos IB, Pereira AP de A, de Souza AJ, Cardoso EJBN, da Silva FG, Oliveira JTC, Verdi MCQ, Sobral JK (2021) Selection and characterization of *Burkholderia* spp. for their plant-growth promoting effects and influence on maize seed germination. Front soil sci 1:805094. https://doi.org/10.3389/fsoil.2021.805094

Duan G, Li L (2023) Deciphering the mechanism of jujube vinegar on hyperlipoidemia through gut microbiome based on 16S rRNA, BugBase analysis, and the stamp analysis of KEEG. Front Nutr 10:1160069. https://doi.org/10.3389/fnut.2023.1160069

Ducret V, Gonzalez MR, Leoni S, Valentini M, Perron K (2020) The CzcCBA efflux system requires the CadA P-type ATPase for timely expression upon zinc excess in Pseudomonas aeruginosa. Front Microbiol 11:911. https://doi.org/10.3389/fmicb.2020.00911

Ducret V, Abdou M, Goncalves Milho C, Leoni S, Martin-Pelaud O, Sandoz A, Segovia Campos I, Lou T-W, Valentini M, Perron K (2021) Global analysis of the zinc homeostasis network in *Pseudomonas aeruginosa* and its gene expression dynamics. Front Microbiol 12:739988. https://doi.org/10.3389/fmicb.2021.739988

Fakhar A, Gul B, Gurmani AR, Khan SM, Ali S, Sultan T, Chaudhary HJ, Rafique M, Rizwan M (2022) Heavy metal remediation and resistance mechanism of Aeromonas, Bacillus, and Pseudomonas: a review. Crit Rev Environ Sci Technol 52:1868–1914. https://doi.org/10.1080/10643389.2020.1863112

Galisteo C, de la Haba RR, Sánchez-Porro C, Ventosa A (2023) A step into the rare biosphere: genomic features of the new genus Terrihalobacillus and the new species Aquibacillus salsiterrae from hypersaline soils. Front Microbiol 14:1192059. https://doi.org/10.3389/fmicb.2023.1192059

Gamalero E, Glick BR (2024) Use of plant growth-promoting bacteria to facilitate phytoremediation. AIMS Microbiol 10:415–448. https://doi.org/10.3934/microbiol.2024021

Ganesh J, Hewitt K, Devkota AR, Wilson T, Kaundal A (2024) IAA-producing plant growth promoting rhizobacteria from Ceanothus velutinus enhance cutting propagation efficiency and Arabidopsis biomass. Front Plant Sci 15:1374877. https://doi.org/10.3389/fpls.2024.1374877

Gendy S, Chauhan A, Agarwal M, Pathak A, Rathore RS, Jaswal R (2020) Is long-term heavy metal exposure driving carriage of antibiotic resistance in environmental opportunistic pathogens: a comprehensive phenomic and genomic assessment using Serratia sp. SRS-8-S-2018. Front Microbiol 11:1923. https://doi.org/10.3389/fmicb.2020.01923

Gilbert NE, Muratore D, Shopen Gochev C, LeCleir GR, Cagle SM, Pound HL, Sun CL, Carrillo A, Ndlovu KS, Maidanik I, Coenen AR, Chittick L, DeBruyn JM, Buchan A, Lindell D, Sullivan MB, Weitz JS, Wilhelm SW (2025) Seasonal enhancement of the viral shunt catalyzes a subsurface oxygen maximum in the Sargasso Sea. bioRxiv. https://doi.org/10.1101/2025.01.23.634377

Gogoi A, Borah N, Nath R (2024) Plant growth-promoting bacteria (PGPB): a potent source of heavy metal stress management in plants. Curr. World Environ 18:1298–1311. https://doi.org/10.12944/cwe.18.3.30

González Henao S, Ghneim-Herrera T (2021) Heavy metals in soils and the remediation potential of bacteria associated with the plant microbiome. Front Environ Sci 9:604216. https://doi.org/10.3389/fenvs.2021.604216

Guzmán-Moreno J, García-Ortega LF, Torres-Saucedo L, Rivas-Noriega P, Ramírez-Santoyo RM, Sánchez-Calderón L, Quiroz-Serrano IN, Vidales-Rodríguez LE (2022) *Bacillus megaterium* HgT21: a promising metal multiresistant plant growth-promoting bacteria for soil biorestoration. Microbiol Spectr 10:1–21. https://doi.org/10.1128/spectrum.00656-22

Halder U, Biswas R, Kabiraj A, Deora R, Let M, Roy RK, Chitikineni A, Majhi K, Sarkar S, Dutta B, Laha A, Datta A, Khan D, Varshney RK, Saha D, Chattopadhyay S, Bandopadhyay R (2022) Genomic, morphological, and biochemical analyses of a multi-metal resistant but multi-drug susceptible strain of *Bordetella petrii* from hospital soil. Sci Rep 12:8439. https://doi.org/10.1038/s41598-022-12435-7

Hamzah Saleem M, Usman K, Rizwan M, Al Jabri H, Alsafran M (2022) Functions and strategies for enhancing zinc availability in plants for sustainable agriculture. Front Plant Sci 13:1033092. https://doi.org/10.3389/fpls.2022.1033092

Hu X, Wang J, Lv Y, Liu X, Zhong J, Cui X, Zhang M, Ma D, Yan X, Zhu X (2021) Effects of heavy metals/metalloids and soil properties on microbial communities in farmland in the vicinity of a metals smelter. Front Microbiol 12:707786. https://doi.org/10.3389/fmicb.2021.707786

Huang SS, Liao QL, Hua M, Wu XM, Bi KS, Yan CY, Chen B, Zhang XY (2007) Survey of heavy metal pollution and assessment of agricultural soil in Yangzhong district, Jiangsu Province, China. Chemosphere 67:2148–2155. https://doi.org/10.1016/j.chemosphere.2006.12.043

Huo Y, Kang JP, Ahn JC, Kim YJ, Piao CH, Yang DU, Yang DC (2021) Siderophore-producing rhizobacteria reduce heavy metal-induced oxidative stress in *Panax ginseng* Meyer. J Ginseng Res 45:218–227. https://doi.org/10.1016/j.jgr.2019.12.008

Hwang JS, Song HG (2020) Antifungal activity of *Bacillus subtilis* isolates against toxigenic fungi. Korean J Microbiol 56:28–35. https://doi.org/10.7845/kjm.2020.0011

Khatoon Z, Orozco-Mosqueda M, Santoyo G (2024) Microbial contributions to heavy metal phytoremediation in agricultural soils: a review. Microorganisms 12:1945. https://doi.org/10.3390/microorganisms12101945

Kim B, Park AR, Song CW, Song H, Kim JC (2022) Biological control efficacy and action mechanism of Klebsiella pneumoniae JCK-2201 producing meso-2,3-butanediol against tomato bacterial wilt. Front Microbiol 13:914589. https://doi.org/10.3389/fmicb.2022.914589

Korean Ministry of Environment (2018) Korean standard soil analysis method, revised in 2018. http://me.go.kr/home/web/law/read.do?pagerOffset=0&maxPageItems=10&maxIndexPages=10&searchKey=lawTitle&searchValue=%ED%86%A0%EC%96%91&menuId=71&orgCd=&condition.typeCode=admrul&typeCode=admrul&lawSeq=586. Accessed 16 January 2023

Kusale SP, Attar YC, Sayyed RZ, El Enshasy H, Hanapi SZ, Ilyas N, Elgorban AM, Bahkali AH, Marraiki N (2021) Inoculation of klebsiella variicola alleviated salt stress and improved growth and nutrients in wheat and maize. Agronomy 11:927. https://doi.org/10.3390/agronomy11050927

Lear L, Padfield D, Hesse E, Kay S, Buckling A, Vos M (2023) Copper reduces the virulence of bacterial communities at environmentally relevant concentrations. Environ Int 182:108295. https://doi.org/10.1016/j.envint.2023.108295

Lee SY, Cho K-S (2025) Plant growth-promoting *Burkholderia* sp. ZF6 enhances heavy metal tolerance in *Brassica juncea* through heavy metal tolerance genes. World J Microbiol Biotechnol 41:191. https://doi.org/10.1007/s11274-025-04429-0

Lee YY, Seo Y, Ha M, Lee J, Yang H, Cho KS (2021) Evaluation of rhizoremediation and methane emission in diesel-contaminated soil cultivated with tall fescue (*Festuca arundinacea*). Environ Res 194:110606. https://doi.org/10.1016/j.envres.2020.110606

Lee YY, Lee SY, Cho KS (2023) Phytoremediation and bacterial community dynamics of diesel- and heavy metal-contaminated soil: long-term monitoring on a pilot scale. Int Biodeterior Biodegrad 183:105642. https://doi.org/10.1016/j.ibiod.2023.105642

Lee SY, Lee Y-Y, Cho K-S (2024) Inoculation effect of heavy metal tolerant and plant growth promoting rhizobacteria for rhizoremediation. Int J Environ Sci Technol 21:1419–1434. https://doi.org/10.1007/s13762-023-05078-2

Li Z, Henawy AR, Halema AA, Fan Q, Duanmu D, Huang R (2022) A wild rice rhizobacterium Burkholderia cepacia BRDJ enhances nitrogen use efficiency in rice. Int J Mol Sci 23:10769. https://doi.org/10.3390/ijms231810769

Li L, Meng D, Yin H, Zhang T, Liu Y (2023) Genome-resolved metagenomics provides insights into the ecological roles of the keystone taxa in heavy-metal-contaminated soils. Front Microbiol 14:1203164. https://doi.org/10.3389/fmicb.2023.1203164

Li B, Feng L, Chouari R, Samoili S, Giannakis S (2025) Trace metals induce microbial risk and antimicrobial resistance in biofilm in drinking water. NPJ Clean Water 8:8. https://doi.org/10.1038/s41545-025-00436-8

Liao Y, Li Z, Yang Z, Wang J, Li B, Zu Y (2023) Response of Cd, Zn translocation and distribution to organic acids heterogeneity in *Brassica juncea* L. Plants 12:479. https://doi.org/10.3390/plants12030479

Liu M, Philp J, Wang Y, Hu J, Wei Y, Li J, Ryder M, Toh R, Zhou Y, Denton MD, Wu Y, Yang H (2022) Plant growth-promoting rhizobacteria *Burkholderia vietnamiensis* B418 inhibits root-knot nematode on watermelon by modifying the rhizosphere microbial community. Sci Rep 12:8381. https://doi.org/10.1038/s41598-022-12472-2

Liu L, Quan S, Li L, Lei G, Li S, Gong T, Zhang Z, Hu Y, Yang W (2024a) Endophytic bacteria improve bio- and phytoremediation of heavy metals. Microorganisms 12:2137. https://doi.org/10.3390/microorganisms12112137

Liu L, Xiao C, Gao Y, Jiang T, Xu K, Chen J, Lin Z, Chen J, Tian S, Lu L (2024b) Inoculation of multi-metal-resistant *Bacillus* sp. to a hyperaccumulator plant *Sedum alfredii* for facilitating phytoextraction of heavy metals from contaminated soil. Chemosphere 366:143464. https://doi.org/10.1016/j.chemosphere.2024.143464

Long Z, Huang Y, Zhang W, Shi Z, Yu D, Chen Y, Liu C, Wang R (2021) Effect of different industrial activities on soil heavy metal pollution, ecological risk, and health risk. Environ Monit Assess 193:1–12. https://doi.org/10.1007/s10661-020-08807-z

Lu M, Li Z, Liang J, Wei Y, Rensing C, Wei G (2016) Zinc resistance mechanisms of P 1B-type ATPases in *Sinorhizobium meliloti* CCNWSX0020. Sci Rep 6:29355. https://doi.org/10.1038/srep29355

Małecka A, Konkolewska A, Hanć A, Ciszewska L, Staszak AM, Jarmuszkiewicz W, Ratajczak E (2021) Activation of antioxidative and detoxificative systems in *Brassica juncea* L. plants against the toxicity of heavy metals. Sci Rep 11:22345. https://doi.org/10.1038/s41598-021-01827-w

Manzoor M, Abid R, Rathinasabapathi B, De Oliveira LM, da Silva E, Deng F, Rensing C, Arshad M, Gul I, Xiang P, Ma LQ (2019) Metal tolerance of arsenic-resistant bacteria and their ability to promote plant growth of *Pteris vittata* in Pb-contaminated soil. Sci Total Environ 660:18–24. https://doi.org/10.1016/j.scitotenv.2019.01.013

Mapanda F, Mangwayana EN, Nyamangara J, Giller KE (2005) The effect of long-term irrigation using wastewater on heavy metal contents of soils under vegetables in Harare, Zimbabwe. Agric Ecosyst Environ 107:151–165. https://doi.org/10.1016/j.agee.2004.11.005

McCorquodale-Bauer K, Flores Orozco D, Grosshans R, Zvomuya F, Cicek N (2025) Reduction of antimicrobial resistance genes in wastewater through phytoremediation. Front Synth Biol 2:1513580. https://doi.org/10.3389/fsybi.2024.1513580

Mohite B (2013) Isolation and characterization of indole acetic acid (IAA) producing bacteria from rhizospheric soil and its effect on plant growth. J Soil Sci Plant Nutr 13:638–649. https://doi.org/10.4067/S0718-95162013005000051

Muratova A, Golubev S, Romanova V, Sungurtseva I, Nurzhanova A (2023) Effect of heavy-metal-resistant PGPR inoculants on growth, rhizosphere microbiome and remediation potential of *Miscanthus* × *giganteus* in zinc-contaminated soil. Microorganisms 11:1516. https://doi.org/10.3390/microorganisms11061516

Nagarajkumar M, Bhaskaran R, Velazhahan R (2004) Involvement of secondary metabolites and extracellular lytic enzymes produced by *Pseudomonas fluorescens* in inhibition of *Rhizoctonia solani*, the rice sheath blight pathogen. Microbiol Res 159:73–81. https://doi.org/10.1016/j.micres.2004.01.005

Niegowska M, Sanseverino I, Navarro A, Lettieri T (2021) Knowledge gaps in the assessment of antimicrobial resistance in surface waters. FEMS Microbiol Ecol 97:1–17. https://doi.org/10.1093/femsec/fiab140

Nnaji ND, Anyanwu CU, Miri T, Onyeaka H (2024) Mechanisms of heavy metal tolerance in bacteria: a review. Sustainability (Switzerland) 16:11124. https://doi.org/10.3390/su162411124

Oliveira TJM, Nascimento VR, Figueiredo ELP, Monteiro LRM, Barros LTC, Nogueira GAS, Freitas JMN, Barbosa AVC, Nascimento ME, Oliveira Neto CF (2024) Phytoremediation potential of Brazilian mahogany (*Swietenia macrophylla* King) on exposure to nickel: anatomical, biochemical and antioxidant responses. Braz J Biol 84:e281527. https://doi.org/10.1590/1519-6984.281527

Phurailatpam L, Dalal VK, Singh N, Mishra S (2022) Heavy metal stress alleviation through omics analysis of soil and plant microbiome. Front Sustain Food Syst 5:817932. https://doi.org/10.3389/fsufs.2021.817932

Prabhakaran R, Thamarai R (2024) Elucidation of the *Cad*A protein 3D structure and affinity for metals. Bioinform Biol Insights 18:1. https://doi.org/10.1177/11779322241266701

Qin H, Wang Z, Sha W, Song S, Qin F, Zhang W (2024) Role of plant-growth-promoting rhizobacteria in plant machinery for soil heavy metal detoxification. Microorganisms 12:700. https://doi.org/10.3390/microorganisms12040700

Raza A, Habib M, Kakavand SN, Zahid Z, Zahra N, Sharif R, Hasanuzzaman M (2020) Phytoremediation of cadmium: physiological, biochemical, and molecular mechanisms. Biology (Basel) 9:1–46. https://doi.org/10.3390/biology9070177

Rensing C, Mitra B, Rosen BP (1997) The *zntA* gene of *Escherichia coli* encodes a Zn(II)-translocating P-type ATPase. Proc Natl Acad Sci USA 94:14326–14331. https://doi.org/10.1073/pnas.94.26.14326

Royet K, Kergoat L, Lutz S, Oriol C, Parisot N, Schori C, Ahrens CH, Rodrigue A, Gueguen E (2025) High-throughput Tn-Seq screens identify both known and novel *Pseudomonas putida* KT2440 genes involved in metal tolerance. Environ Microbiol 27:e70095. https://doi.org/10.1111/1462-2920.70095

Schmittgen TD, Livak KJ (2008) Analyzing real-time PCR data by the comparative CT method. Nat Protoc 3:1101–1108. https://doi.org/10.1038/nprot.2008.73

Schwager S, Lumjiaktase P, Stöckli M, Weisskopf L, Eberl L (2012) The genetic basis of cadmium resistance of *Burkholderia cenocepacia*. Environ Microbiol Rep 4:562–568. https://doi.org/10.1111/j.1758-2229.2012.00372.x

Singh S, Parihar P, Singh R, Singh VP, Prasad SM (2016) Heavy metal tolerance in plants: role of transcriptomics, proteomics, metabolomics, and ionomics. Front Plant Sci 6:1143. https://doi.org/10.3389/fpls.2015.01143

Śliwa-Cebula M, Kaszycki P, Kaczmarczyk A, Nosek M, Lis-Krzyścin A, Miszalski Z (2020) The common ice plant (*Mesembryanthemum crystallinum* l.)–phytoremediation potential for cadmium and chromate-contaminated soils. Plants 9:1–18. https://doi.org/10.3390/plants9091230

Sun T, Delaplace P, Li G, James A, Pan J, Zhang J (2025) Novel insights into the effect of arbuscular mycorrhizal fungi inoculation in soils under long-term biosolids application: emphasis on antibiotic and metal resistance genes, and mobile genetic elements. Environ Pollut 369:125846. https://doi.org/10.1016/j.envpol.2025.125846

Syed A, Elgorban AM, Bahkali AH, Eswaramoorthy R, Iqbal RK, Danish S (2023) Metal-tolerant and siderophore producing *Pseudomonas fluorescence* and *Trichoderma* spp. improved the growth, biochemical features and yield attributes of chickpea by lowering Cd uptake. Sci Rep 13:4471. https://doi.org/10.1038/s41598-023-31330-3

Taeprayoon P, Pongphontong K, Somtrakoon K, Phusantisampan T, Meeinkuirt W (2024) Synergistic effects of zinc and cadmium on phytoremediation potential of Christmas moss (*Vesicularia montagnei*). Sci Rep 14:17754. https://doi.org/10.1038/s41598-024-68849-y

Wang G, Zhang Q, Du W, Ai F, Yin Y, Ji R, Guo H (2021) Microbial communities in the rhizosphere of different willow genotypes affect phytoremediation potential in Cd contaminated soil. Sci Total Environ 769:145224. https://doi.org/10.1016/j.scitotenv.2021.145224

Wang Y, Narayanan M, Shi X, Chen X, Li Z, Natarajan D, Ma Y (2022) Plant growth-promoting bacteria in metal-contaminated soil: current perspectives on remediation mechanisms. Front Microbiol 13:966226. https://doi.org/10.3389/fmicb.2022.966226

Wang C, Yu QY, Ji NN, Zheng Y, Taylor JW, Guo LD, Gao C (2023) Bacterial genome size and gene functional diversity negatively correlate with taxonomic diversity along a pH gradient. Nat Commun 14:7437. https://doi.org/10.1038/s41467-023-43297-w

Wang Z, Hülpüsch C, Foesel B, Traidl-Hoffmann C, Reiger M, Schloter M (2024) Genomic and functional divergence of *Staphylococcus aureus* strains from atopic dermatitis patients and healthy individuals: insights from global and local scales. Microbiol Spectr 12:1–19. https://doi.org/10.1128/spectrum.00571-24

Wu X, Su N, Yue X, Fang B, Zou J, Chen Y, Shen Z, Cui J (2021) IRT1 and ZIP2 were involved in exogenous hydrogen-rich water-reduced cadmium accumulation in *Brassica chinensis* and *Arabidopsis thaliana*. J Hazard Mater 407:124599. https://doi.org/10.1016/j.jhazmat.2020.124599

Yahaya SM, Abubakar F, Abdu N (2021) Ecological risk assessment of heavy metal-contaminated soils of selected villages in Zamfara State, Nigeria. SN Appl Sci. https://doi.org/10.1007/s42452-021-04175-6

Yang J, Guo Z, Al-Dhabi NA, Shi J, Peng Y, Miao B, Liu H, Liang Y, Yin H, Liu X, Tang W, Jiang L (2024) The succession of microbial community and distribution resistance gene in response to enrichment cultivation derived from a long-term toxic metal(loid)s polluted soil. Sci Total Environ 954:176385. https://doi.org/10.1016/j.scitotenv.2024.176385

Yu X, Zhao JT, Liu X, Sun LX, Tian J, Wu N (2021) Cadmium pollution impact on the bacterial community structure of arable soil and the isolation of the cadmium resistant bacteria. Front Microbiol 12:698834. https://doi.org/10.3389/fmicb.2021.698834

Zhang Q, Wang L, Xu D, Tao Z, Li J, Chen Y, Cheng Z, Tang X, Wang S (2023a) Accelerated Pb(II) removal and concurrent bioelectricity production via constructed wetland-microbial fuel cell: structural orthogonal optimization and microbial response mechanism. J Water Process Eng 56:104287. https://doi.org/10.1016/j.jwpe.2023a.104287

Zhang Y, Jiang Y, Gao K, Sui D, Yu P, Su M, Wei GW, Hu J (2023b) Structural insights into the elevator-type transport mechanism of a bacterial ZIP metal transporter. Nat Commun 14:385. https://doi.org/10.1038/s41467-023-36048-4

Zhou G, Liu C, Cheng Y, Ruan M, Ye Q, Wang R, Yao Z, Wan H (2022) Molecular evolution and functional divergence of stress-responsive Cu/Zn superoxide dismutases in plants. Int J Mol Sci 23:7082. https://doi.org/10.3390/ijms23137082

Zhu S, Mao H, Yang X, Zhao W, Sheng L, Sun S, Du X (2025) Resilience mechanisms of rhizosphere microorganisms in lead-zinc tailings: metagenomic insights into heavy metal resistance. Ecotoxicol Environ Saf 292:117956. https://doi.org/10.1016/j.ecoenv.2025.117956

Publisher's Note Springer Nature remains neutral with regard to jurisdictional claims in published maps and institutional affiliations.